

# DETERMINATION OF SCOUR DEPTH IN SUBMARINE PIPELINES

By

Akshay Ramesh Mathur



College of Engineering  
University of Petroleum & Energy Studies  
Dehradun  
May, 2015

# DETERMINATION OF SCOUR DEPTH IN SUBMARINE PIPELINES

A thesis submitted in partial fulfilment of the requirements for the Degree of  
Master of Technology  
(Pipeline Engineering)

By  
Akshay Ramesh Mathur

Under the guidance of

Mr. Adarsh K. Arya  
Asst. Professor,  
Department of Chemical Engineering  
University of Petroleum and Energy Studies, Dehradun

Approved by

Dr. Kamal Bansal  
Dean

College of Engineering  
University of Petroleum & Energy Studies  
Dehradun  
May, 2015

## **CERTIFICATE**

This is to certify that the work contained in this thesis titled “Determination of scour depth in submarine pipelines” has been carried out by Akshay Ramesh Mathur under my supervision and has not been submitted elsewhere for a degree.

Mr. Adarsh K. Arya  
Asst. Professor,  
Dept. of Chemical Engineering,  
U.P.E.S, Dehradun

Date : 01 May, 2015

## **ACKNOWLEDGEMENT**

Every project, big or small, is successful largely due to the effort of a number of wonderful people who have always given their valuable advice and guidance. I sincerely appreciate the inspiration, support and guidance of all those people who have been instrumental in making this project a success.

I take this opportunity to express my profound gratitude and deep regards to my guide, Mr. Adarsh K. Arya, Asst. Professor, Dept. of Chemical Engineering, for giving me the opportunity to carry out this project and for his exemplary guidance, monitoring and constant encouragement throughout my post-graduate course. The blessing, help and guidance given by him time to time shall carry me a long way in the professional journey on which I am about to embark.

I am also thankful to Dr. Kamal Bansal, Dean, College of Engineering Studies, for providing me with a platform to enhance my knowledge and for his eternal inputs and motivation.

I would also like to thank all the faculty members of University of Petroleum and Energy Studies for their critical advice and guidance throughout my post-graduation course.

Lastly, I place a deep sense of gratitude to my family members and my friends who have been a constant source of inspiration during the preparation of this project work.

## **ABSTRACT**

The rapid development of offshore oil fields has led to an increase in the construction of submarine pipelines for transport of crude oil to onshore refineries. The interactions between the pipeline and an erodible bed under current and/or wave conditions tend to cause scouring below the pipeline. Scour underneath the pipeline may cause long sections of the pipeline to suspend in water. If the free span of the section is long enough, the pipeline section affected by scour may experience resonant flow-induced oscillations, leading to structural failure. Therefore, accurate estimates of the scour depth are important in the design of submarine pipelines. At present, several empirical methods, based on various research findings, can be found in literatures for estimating the equilibrium scour depth under both current and wave conditions. Experiments for predicting the behavior of submarine pipelines on an erodible seabed have also been carried out based upon a series of flume tests with current and waves. The project deals with the review of previous research works and comparison of the experimental results with the results obtained from the empirical equations to obtain the most accurate method of calculating the scour depth below submarine pipelines. Methods to mitigate scour have also been summarized. The critical parameters which have to be considered for the minimization of the equilibrium scour depth have been discussed.

## TABLE OF CONTENTS

CERTIFICATE.....	iii
ACKNOWLEDGEMENT .....	iv
ABSTRACT.....	v
LIST OF FIGURES .....	vii
LIST OF TABLES.....	viii
NOMENCLATURE .....	ix
CHAPTER 1: INTRODUCTION.....	1
CHAPTER 2: LITERATURE REVIEW .....	4
CHAPTER 3: THEORETICAL DEVELOPMENT.....	9
3.1 Amplification Factor.....	9
3.2 Equilibrium Scour Depth and the Time Scale of Scour.....	10
3.3 Clear Water Scour and Live Bed Scour .....	11
3.4 Onset of Scour.....	13
3.4.1 Mechanism of onset of scour: Seepage flow and piping underneath the pipe.	15
3.4.2 Parameters affecting the onset of scour process .....	21
3.4.3 Criterion for the onset of scour .....	25
3.5 Tunnel Erosion.....	27
3.6 Lee-wake Erosion .....	28
3.7 Equilibrium Scour Depth Stage .....	29
3.8 Research Work on Equilibrium Scour Depth .....	30
3.9 Scour Prevention and Repair .....	34
3.9.1 Local Methods .....	35
3.9.2 Global Methods.....	39
CHAPTER 4: EXPERIMENTAL FINDINGS.....	41
CHAPTER 5: CALCULATIONS, RESULTS AND DISCUSSIONS .....	45
CHAPTER 6: CONCLUSIONS AND RECOMMENDATIONS .....	65
REFERENCES .....	66
APPENDIX I .....	69

## LIST OF FIGURES

Fig. No.	Figure	Page No.
3.1	Time Development of Scour Depth	10
3.2	Variation of equilibrium scour depth v/s the Shield's parameter	12
3.3	General scour around a pipeline	13
3.4	Formation of three vortices	14
3.5	Onset of scour process	14
3.6	Scour hole under the waves	15
3.7	Seepage flow underneath the pipe	16
3.8	Time series of pressure gradient underneath the pipe: Current case	17
3.9	Piping times corresponding to Fig. 3.8	19
3.10	Time series of pressure gradient underneath the pipe: Wave case	20
3.11	Sequence of flow pictures over one wave cycle	21
3.12	The parameters which describe the flow pattern around the pipe	22
3.13	The parameters which describe the characteristics of the pipe	23
3.14	Parameters of the scour hole	24
3.15	Definition sketch of approach flow	27
3.16	Tunnel erosion below a pipeline	28
3.17	Scour development: Current case	28
3.18	Sediment motion caused by vortex passing overhead	29
3.19	Time development of scour depth: a) Current case, b) Wave case	30
3.20	Anti-Scour Device (ASD)	36
3.21	Sedimentary Deposition Device (SDD)	37
3.22	Glass Fibre Dome (GFD)	38
4.1	Set up for the pressure measurement	41
4.2	Sinking of pipeline at span shoulder	42
5.1	Equilibrium Scour Depth v/s $KC$ number	64

## LIST OF TABLES

Table No.	Table	Page No.
1	Experimental findings for three cases: Case 1: $D = 10$ cm, Case 2: $D = 5$ cm, Case 3: $D = 2$ cm	44
2	Experimental findings for Case 1: $D = 10$ cm	45
3	Experimental findings for Case 2: $D = 5$ cm	47
4	Experimental findings for Case 3: $D = 2$ cm	49
5	Calculation of Average Percentage Error	52
6	Input parameters for $D = 10$ cm, $KC = 8$	53
7	Input parameters for $D = 10$ cm, $KC = 16$	55
8	Input parameters for $D = 5$ cm, $KC = 7$	57
9	Input parameters for $D = 5$ cm, $KC = 30$	58
10	Input parameters for $D = 2$ cm, $KC = 45$	60
11	Input parameters for $D = 2$ cm, $KC = 75$	62
12	Calculation of percentage error for Case 1: $D = 10$ cm	69
13	Calculation of percentage error for Case 2: $D = 5$ cm	70
14	Calculation of percentage error for Case 3: $D = 2$ cm	71

## NOMENCLATURE

VLCC	Very large crude carriers
$KC$	Keulegan-Carpenter number
$S/D$	Non-dimensional scour depth
ANN	Artificial neural networks
$\beta$	Frequency parameter
$\alpha$	Amplification factor
$\tau$	Bed shear stress
$\tau_{\infty}$	Bed shear stress for the undisturbed flow
$S$	Maximum depth of the scour hole
$S_t$	Time scale of the scour process
$T$	Time period
$\theta$	Shield's parameter
$Re$	Reynold's number
$U_f$	Undisturbed bed shear velocity
$g$	Acceleration due to gravity
$s$	Specific gravity of the bed material
$d_{50}$	Mean grain size
$\theta_{cr}$	Critical value of the Shield's parameter
$\nu$	Kinematic viscosity
$D$	Pipeline diameter
$W$	Submerged weight of the sand
$\gamma_s$	Specific weight of the sand grains
$\gamma$	Specific weight of water
$n$	Porosity of the bed material
$\sigma$	Standard deviation
$\eta$	Surface elevation
$U$	Current velocity

$U_*$	Orbital velocity
$H$	Wave height
$h$	Water depth
$r$	Bottom roughness
$e$	Initial gap between the pipeline and the seabed
$\theta_w$	Angle between pipe direction and predominant wave propagation
$\theta_c$	Angle between pipe direction and predominant (tidal) current propagation
$A$	Total amount of eroded sediment
$L_a$	Horizontal distance from vertical pipe axis to sea bottom downstream of the pipe (or in the direction of wave propagation)
$L_v$	Horizontal distance from vertical pipe axis to sea bottom upstream of the pipe (or against the direction of wave propagation)
$k_s/D$	Relative roughness
$a$	Amplitude of the orbital motion of the water particles at the bed
ASD	Anti-scour device
SSD	Sedimentary deposition device
GFD	Glass fibre dome

## CHAPTER 1: INTRODUCTION

A **submarine** pipeline (also known as **marine**, **subsea** or **offshore** pipeline) is a pipeline that is laid on the seabed or below it inside a trench. The rapid development of offshore oil fields has increased the construction of submarine pipelines for transport of crude oil to onshore refineries. They are also used for the disposal of waste water into the seas. It is customary to bury the pipelines to protect them from possible damage caused by waves, currents, and anchor dropping or dragging. However, the cost of trenching and refilling the pipelines is high, and expenditure on pipeline burial often accounts for a large proportion of the total budget of the project. Hence, pipelines are usually laid on the seabed.

When a structure is placed the sandy seabed, the presence of the structure will change the incoming flow. The presence of submarine pipelines alters the dynamics of flow at the seabed. Such pipelines are exposed to wave and current action. The changed flow, due the action of currents and waves, transports sand particles underneath the pipeline away from it, creating a hole around it. This phenomenon is called scour. Water normally flows faster around such submerged pipelines, making them susceptible to local scour. Local scour around submarine pipelines is therefore, a complex phenomenon due to the triple interaction of pipe, bed and flow.

Scour underneath the pipeline may expose parts of the pipe causing it to suspend in water. If the free span of the pipe is long enough, the pipe may experience resonant flow-induced oscillations, leading to structural failure. Accurate estimates of the scour depth are important in the design of submarine pipelines. The results of scour depend on the geometry and material of the seabed, the velocity of the incoming flow and ratio between the orbital fluid particle displacement and the characteristic dimensions of the pipeline.

Hence, one of the most important aspects in pipe design which is laid on a mobile seabed is assessing the stability of the pipeline as a consequence of scour. Scouring process depends on local flow structures, i.e., formation of vortices around submarine pipeline resting on a plane bed. The onset of scour is due to the combined action of the vortices

and under flow, which leads to the formation of a small opening under the pipe as more and more sand particles are carried away. However, in the course of this process, vortex mechanism is going to be changed and finally local transport capacity of the flow around the pipeline will not be enough for carrying the sand particles away because of the scour volume will be sufficiently large, and then scour process will reach a dynamic equilibrium condition. Flow structure for submarine pipelines depends mainly on the Reynolds number, the Keulegan-Carpenter number and also the gap ratio  $e/D$  (where  $e$  is the initial gap between the pipeline and the sea bed).

Therefore it is highly essential to analyze the dynamic responses of a submarine pipeline near the seabed in severe ocean environments for the proper design of submarine pipelines. Hence, the scour process has been mainly studied by using physical modeling (e.g. Lucassen, 1984, Mao, 1986, Sumer and Fredsoe, 1990, Pu et al., 2001, Sumer et al., 2001). In these studies, different relationships have been developed to investigate the scour depth underneath pipelines in different conditions. Numerical methods were developed to simulate the scour around submarine pipelines, e.g. (Liang and Cheng, 2005a, Liang and Cheng, 2005b). However, these methods are very complex and time-consuming. In the last decade, soft computing tools like Artificial Neural Networks (ANNs) and Fuzzy Inference Systems (FIS) have been a powerful technique in ocean engineering fields such as scour depth around piles or pipes (e.g. Kambekar and Deo, 2003, Kazeminezhad et al., 2010). However, these methods disclose very few information regarding the physical processes, and hence they are not as transparent as regression methods.

In this project, the results from an experiment (conducted by Sumer and Fredsøe, 2001) to predict the scour depth are compared with the results obtained from the empirical formulae given by various researchers. A detailed literature review has been carried out, where the previous work done by researchers was reviewed, and this is described in Chapter 2. In Chapter 3, a brief description about the scour process has been outlined, The difference between clear-water and live-bed conditions have been explained, along with the description of the scour process, right from the onset of scour followed by tunnel

erosion, lee-wake erosion and the equilibrium condition. A brief summary on the methods for scour prevention and repair has also been described. In Chapter 4, the experimental setup has been described, with an explanation about the self-burial mechanism. The experimental findings have been tabulated for comparison with the values obtained from empirical equations. In Chapter 5, the scour depth has been calculated using the empirical formulae given by various researchers. In order to identify which empirical formula is the most accurate for predicting the scour depth, comparison is made with the experimental findings and the results obtained from each empirical formula discussed in the theoretical development section. The average percentage error in scour depth calculation has been found out for each empirical equation to determine the most accurate method to predict the scour depth. The most accurate equations have been then used to calculate the equilibrium scour depth for different pipe diameters, by changing the governing parameters. The variation of equilibrium scour depth with respect to the Keulegan – Carpenter number has been established. In Chapter 6, conclusions and recommendations for future work have been discussed.

## CHAPTER 2: LITERATURE REVIEW

Many researchers have carried out research in the field of scour prediction and detection under submarine pipelines. The first of the investigations to determine scour depth was conducted by Kjeldsen et al. in 1973. Ibrahim and Nalluri (1986) proposed empirical equations relating scour depth to flow parameters. Sumer and Fredsøe developed empirical equations based on experimental findings. A summary of the previous research work carried out has been given below.

Kjeldsen et al. in 1973 conducted flume experiments to investigate local scour around submarine pipelines under unidirectional current. They proposed an empirical equation relating the scour depth to the velocity head and the pipe diameter. The work carried out by Kjeldsen et al. was the basis on which future research was carried out. The equation implies that the scour depth depends only on the flow velocity and the pipe diameter, but excludes other parameters such as flow depth and grain size, which also have a considerable effect on the scour depth.

Bijker and Leeuwestein in 1984 predicted the behavior of submarine pipelines on an erodible seabed based on a series of small scale flume tests with currents and waves. The research was carried out at the Delft University of Technology, Netherlands, They studied the influence of basic parameters such as pipe diameter, approach velocity and height of the pipe relative to the original seabed. The process of scour around pipelines due to current and wave action has been explained in the study. They also explained the different types of erosion occurring at the seabed. They used the datasets of the experiments carried out by Kjeldsen (1974), van Ast and de Boer (1973) and many others for comparison with their experimental results.

Lucassen in 1984 conducted physical experiments on scour under submarine pipelines in the laboratory for fluid mechanics in Delft University of Technology, Netherlands. Experiments were carried out for three cases: scour due to action of currents, scour due to action of waves, and scour due to combined action of currents and waves. Results were

documented for different sediment sizes and the influence of the mean grain size on the scour process was investigated. It was shown that scour due to waves is of minor importance compared to the scour due to current. Also, for coarse sediment the scour depth due to waves was found to be independent of the pipe diameter. For fine sediment, the scour depth was found to be independent of the wave period and proportional with the pipe diameter. A linear relationship between the scour depth and the undisturbed maximum orbital velocity near the bottom was established.

Ibrahim and Nalluri in 1986 conducted an extensive experimental program on local scour around submarine pipeline conducted at the University of Newcastle upon Tyne. They proposed two equations, one each for clear water and live bed conditions respectively. They reviewed the work carried out by Kjeldsen et al. (1973) and stated that the scour depth is related not only with flow velocity and pipe diameter but also the flow depth. However, they were not able to clarify how exactly the flow depth affected the equilibrium scour depth, because they derived the equations purely from curve-fitting technique without due considerations to the physics describing the scouring process.

Sumer and Fredsøe in 1991 carried out experiments in a wave flume to investigate the onset of scour and the presence of tunnel erosion. The study focused on the parameters such as initial burial depth and the Keulegan-Carpenter number. They showed that the critical burial depth beyond which no scour occurs is a function of the  $KC$  number. The mechanism of onset of scour was explained in detail. They showed that the onset of scour underneath a partially buried pipe occurred under the combined action of the vortices that form on the upstream and downstream sides of the pipe and the pressure gradient that builds up through the sand bed across the pipe due to the pressure difference between the upstream and downstream sides of the pipe.

Cheiw in 1991 proposed an empirical equation relating the amount of gap flow through the scour hole for given flow conditions. Using this, he predicted the maximum scour depth underneath submarine pipelines for a given flow and geometric boundary conditions. The results suggested that the maximum equilibrium scour depth occurs when

the pipeline is just lying on a plane bed and subjected to a pure unidirectional current. It was assumed that there is no general sediment transport away from the pipeline. The predicted maximum scour depth compared well with the experimental results.

Sumer et al. in 1992 developed a non-dimensional formula to calculate the time scale of the scour process below a marine pipeline, based on the available data for both current and wave conditions. It was found that the time scale of the scour process below a pipeline is governed by the Shield's parameter. The results indicated that the non-dimensional time scale is proportional to the  $-5/3$  power of the Shield's parameter. In the study, the time scale of scour involving a change in wave climate was also investigated. It was found that the time scale is governed by the Shield's parameter plus the two Keulegan-Carpenter numbers corresponding to the waves before and after the change takes place.

Cevik and Yuksel in 1997 carried out experiments to determine the scour depth below submarine pipelines placed in a rigid position on the seabed under wave conditions. It was found that the relative scour depth depends on the Keulegan-Carpenter number and frequency parameter ( $\beta$ ). It was found that the relative scour depth is proportional to the frequency parameter and the grain size gradation does not affect the scour depth below submarine pipelines. They developed an empirical equation to predict the scour depth which was almost along the lines of the equation given by Sumer and Fredsøe (1990).

Qin, C in 1998 conducted a scour test for sagging pipes to calculate the erosive depth and limit for various water depth, wave parameters, pipe diameter and sand size. Using the wave theory, he showed the vortex intensity in front and back of the pipe is related to the Keulegan-Carpenter number at two points. The study considered that erosive limit and erosive hole depth is related to the wave character, pipe diameter, pipe feature and sand size at the seabed. Based on the experimental findings, he proposed a semi-theory and semi-experimental expression of relative depth of the erosive hole as a function of difference between the  $KC$  numbers obtained at the two points. In other words, he

established that the erosive hole size was essentially the function of the momentum difference at the top of the pipe and its bottom.

Sumer et al. in 2001 conducted an experimental study on the onset of scour below submarine pipelines and its self-burial in under the action of currents and waves. The experimental dataset is used in this project to compare with the results obtained from empirical formulae suggested by various researchers. It was shown that the onset of scour was a result of piping; the excessive seepage flow underneath the pipe due to the pressure difference between the upstream and downstream sides of a pipeline. Secondary effects such as vortices were found to be agitating forces for the piping process. For both current and wave conditions, the critical parameters and critical conditions for onset of scour were determined. The equilibrium self-burial depth was also found out for both current and wave conditions.

Etemad-Shahidi et al. in 2010 used Artificial Neural Networks (ANNs) to increase the accuracy of the scour depth prediction. The wave-induced scour was studied in both clear water and live bed conditions. Several dimensionless parameters such as gap to diameter ratio, Keulegan-Carpenter number and Shields number were used. The results showed that the ANN models increased the accuracy of the scour prediction and that the Shields number is a very important parameter in the clear water condition. To establish an empirical formula for predicting the scour depth, databases for development of the formulae were collected from the existing experimental studies in different conditions. Using ANN model trees, they suggested empirical equations for predicting the scour depth in both live bed and clear water conditions. They also suggested an empirical equation to determine the critical Shield's number, which is the basis for distinguishing between clear water and live-bed conditions.

Yasa, R. in 2011 studied the scour around submarine pipelines over an erodible bed under wave conditions. An empirical formula was proposed using multiple regression analysis to predict the wave-induced scour depth. The effect of  $KC$  number and pipe initial gap on

the equilibrium scour depth was investigated. The significant correlation between  $KC$  number,  $e/D$ ,  $\theta$  and the non-dimensional scour depth ( $S/D$ ) was established.

T. N. Watson in 1974 studied the various methods available for protecting permanent offshore structures against scour. Techniques involving Anti-Scour Device (ASD), Sediment Deposition Device (SDD), gravel deposition, use of sea-carpets, artificial seaweed, fabriform process, etc. were described in the study. Also, comparisons between the different techniques were made to identify the most viable option considering the transportation, installation, maintenance and monitoring costs and efficiency.

Angus N. and Moore R. in 1982 suggested methods for scour repair in the Southern North Sea. The various factors affecting the formation of scour and the effect of scour on pipeline stability was described, followed by describing several methods carried out to prevent or repair scour.

## **CHAPTER 3: THEORETICAL DEVELOPMENT**

When a pipeline is placed in the marine environment, the presence of the pipeline will change the flow pattern in its immediate neighborhood, resulting in one or more of the following phenomena:

1. The contraction of flow;
2. The formation of a horseshoe vortex in front of the structure;
3. The formation of lee-wake vortices behind the structure;
4. The generation of turbulence;
5. The occurrence of reflection and diffraction of waves;
6. The occurrence of wave breaking; and
7. The pressure differentials in the soil that may produce “quick” condition or liquefaction allowing material to be carried off by currents.

These changes usually cause an increase in the local sediment transport capacity and thus lead to scour. The scour is a threat to the stability of the pipeline.

Such pipelines are usually exposed to currents, waves and combined waves and currents.

### **3.1 Amplification Factor**

Consider a pipeline placed in a marine environment. The presence of the pipeline will cause the flow in its neighborhood to change. This local change in the flow will generally cause an increase in the bed shear stress and in the turbulence level. The sediment transport close to the pipeline is increased mainly because:

1. The average bed shear stress is increased close to the pipeline, and
2. The degree of turbulence is increased in the vicinity of the pipeline.

Both features will lead to an increase in the local sediment transport capacity. However, the increase in average bed shear stress is the more prominent factor.

Usually the increase in the bed shear stress is expressed in terms of the so-called amplification factor defined by:

$$\alpha = \tau / \tau_{\infty} \quad (1)$$

In which  $\tau$  = the bed shear stress and  $\tau_{\infty}$  = the bed shear stress for the undisturbed flow. Owing to the local increase in  $\alpha$  (i.e.  $\alpha > 1$ ), the sediment transport capacity will increase and presumably the bed will be eroded. This process will continue until the scour reaches such levels that the bed shear stress around the pipeline becomes  $\alpha = 0$  as seen in Fig. 3.1. The stage where the scour process comes to an end is called the equilibrium stage.

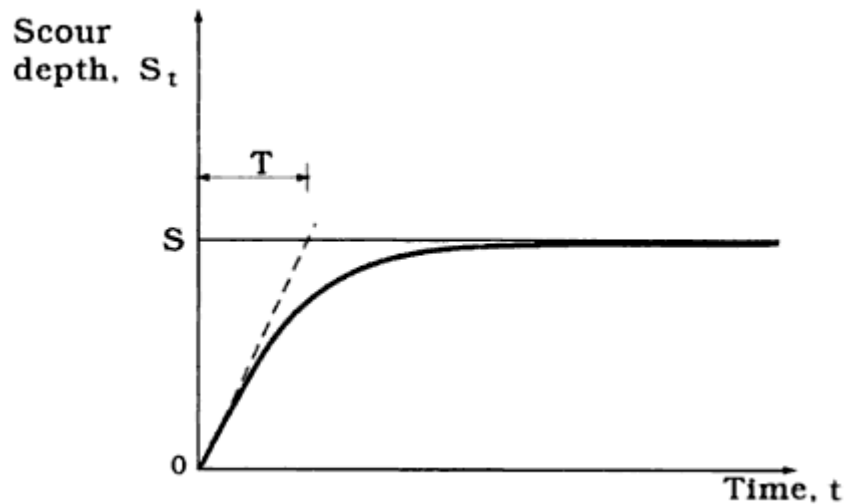


Fig. 3.1: Time development of scour depth <sup>[1]</sup>

### 3.2 Equilibrium Scour Depth and the Time Scale of Scour

The scour develops towards the equilibrium stage through a transitional period, as illustrated schematically in Fig. 3.1. The scour depth corresponding to the equilibrium stage in Fig. 3.1 is called the equilibrium scour depth.

It can be seen from Fig. 3.1 that, for a substantial amount of scour to develop, a certain amount of time must elapse. This time is called the time scale of the scour process. The time scale of the scour process may be defined as follows:

$$S_t = S (1 - \exp (-t / T)) \quad (2)$$

In which  $T$  = the time scale of the scour process, and corresponds to the time period  $T$  indicated in Fig. 3.1 where the dashed line is tangent to the scour depth v/s time curve at  $t = 0$ .

### 3.3 Clear Water Scour and Live Bed Scour

Scour may be classified in two categories: clear water scour and live bed scour. In case of clear water scour, no sediment motion takes place far from the structure ( $\theta < \theta_{cr}$ ), while, in case of live bed scour, the sediment transport prevails over the entire bed ( $\theta > \theta_{cr}$ ). Here  $\theta$  is the undisturbed Shield's parameter which is defined by:  $\tau_{\infty} / \rho$

$$\theta = U_f^2 / [g (s - 1) d_{50}] \quad (3)$$

In which  $U_f = (\tau_{\infty} / \rho)^{0.5}$ , the undisturbed bed shear velocity,  $g$  = acceleration due to gravity,  $s$  = the specific gravity of the bed material and  $d_{50}$  = the grain size.  $\theta_{cr}$  is the critical value of the Shield's parameter corresponding to the initiation of sediment motion at the bed.  $\theta_{cr}$  is function of the grain Reynold's number ( $d \times U_f / \nu$ ).

In the clear water case, the variation of the scour depth with  $\theta$  is more pronounced: as illustrated in Fig. 3.2, the scour depth increases from zero at very small values of  $\theta$  up to  $\theta_{cr}$ . At very low  $\theta$  values, no scour will occur because, in this case, even the amplified local bed shear stress may still be too small to cause sediment transport. However, when the live bed case is reached, and beyond  $\theta > \theta_{cr}$ , a very small variation of the scour depth with  $\theta$  is observed. This is because any change in  $\theta$  results in corresponding changes in

sediment transport, and these changes occur both inside and outside of the scour hole in equivalent amounts, eventually causing only small changes in the equilibrium scour hole.

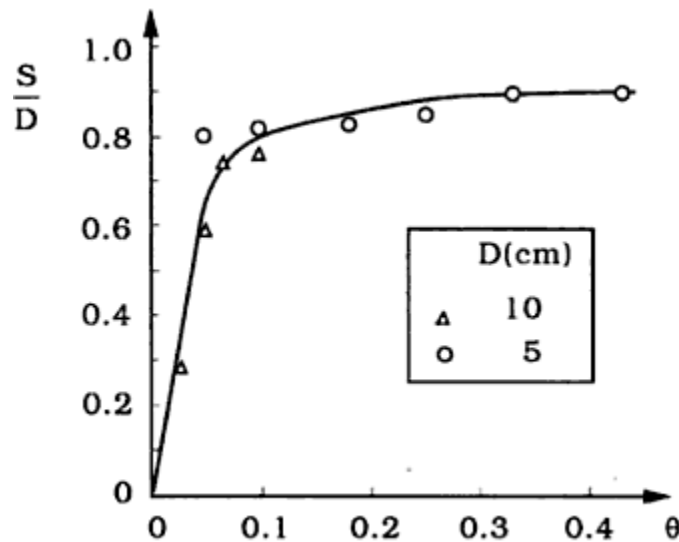


Fig. 3.2: Variation of equilibrium scour depth versus the Shield's parameter <sup>[2]</sup>

Pipelines are a very convenient means to transport oil, gas, water, and waste water along the sea bed. They are used for transportation from offshore platforms to onshore refineries. The developments in the offshore oil and gas industry in recent years has led to tens of thousands of kilometers of submarine pipeline networks laid across the globe, and these networks have become the “lifelines” of the oil and gas industry.

The interaction between a submarine pipeline and an erodible bed is important in the field of offshore and coastal engineering. When a pipeline is exposed to direct flow action and when the seabed is erodible, scour may occur around the pipe under the flow action, which may lead to suspended free spans of the pipeline. The pipeline along the length of the suspended span may or may not sag in the generated scour hole. In the case of a sagging pipeline, the pipeline may reach the bottom of the scour hole, which may be followed by backfilling and eventual self-burial of the pipeline. In either case, the suspended length of the pipeline experiences stresses which may eventually lead to the failure of the pipeline.

### 3.4 Onset of Scour

Scour below pipelines in the field occurs in a three-dimensional fashion: the scour breaks out underneath the pipe locally, and it propagates along the length of the pipeline in both directions as shown in Fig. 3.3. The scour holes formed in this way are interrupted by stretches, called span shoulders, where the pipe obtains its support. However after the process has reached a reasonably developed stage, the scour in the middle part of a scour hole can be considered as a two dimensional process.

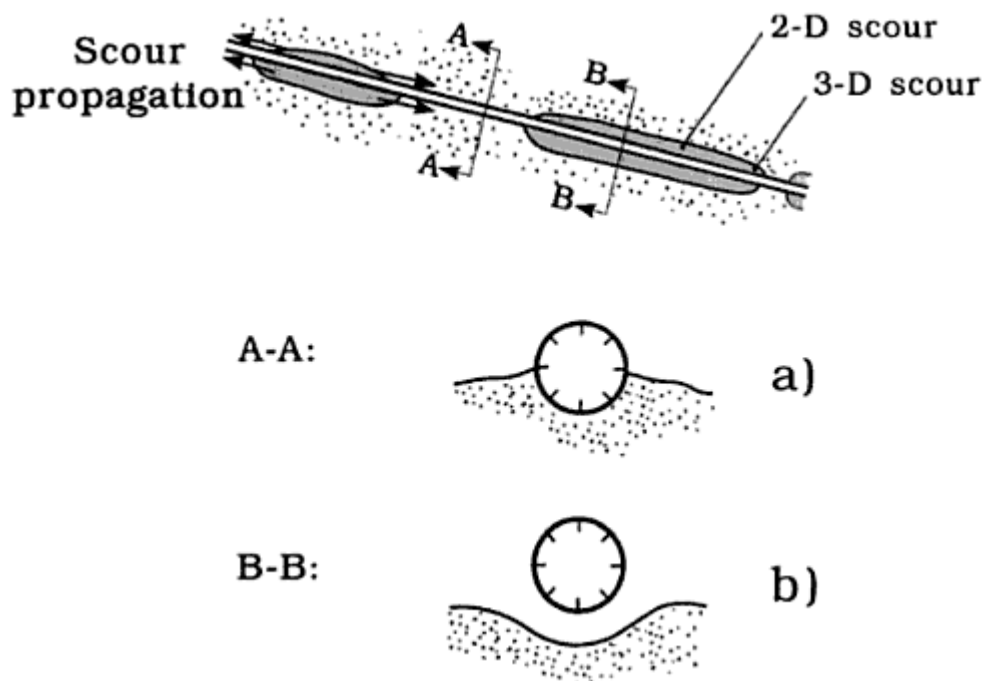


Fig. 3.3: General scour around a pipeline <sup>[3]</sup>

Consider a pipeline laid on an erodible bed. If the initial embedment of the pipeline in the bed is not very large, and the flow (induced by currents/waves) is sufficiently strong, the bed may be washed away underneath the pipe, and the phenomenon is termed as **onset of scour**. The onset of scour is basically related to the seepage flow in the sand beneath the pipeline which is driven by the pressure difference between the upstream and downstream sides of the pipeline.

When a pipe is placed on a plane bed without any opening under the pipe, the originally uniform distribution of the flow field is disturbed by the presence of the pipe. Three vortices are formed in the neighborhood of the resting pipe<sup>[4]</sup>. As shown in Fig. 3.4, vortex A is in front of the pipe. Behind the pipe, flow forms a large vortex B, and in the corner downstream of the pipe, there is a vortex C. Yuksel et al. (1995), however, reported five vortices, two of them formed upstream of the pipe, the other three developing on the downstream side of the pipe<sup>[5]</sup>. In the neighborhood of the pipe, as shown in Fig. 3.5 (a), both vortices A and C move sand particles away from the footing area, but their moving directions are opposite to each other. Conversely, vortex B moves sand particles towards the pipe, but its acting area is limited by vortex C. Due to the combined action of the vortices and the underflow, more and more sand particles are moved away. At last, a small opening is created under the pipe. This process is called as “piping”, and is the onset of scour under a unidirectional flow condition. After the water has started to flow underneath the pipe, the upstream vortex disappears, the velocity in the gap is approximately equal to the one above the pipe, and this relatively high velocity causes strong tunnel erosion.

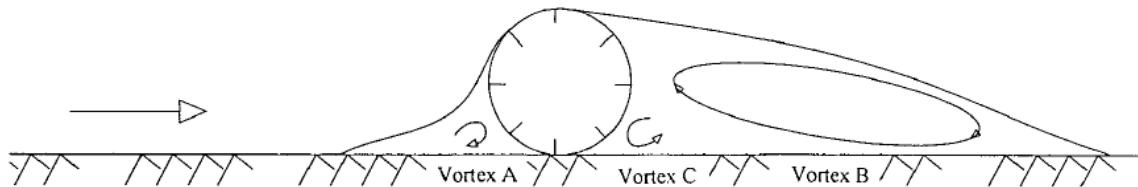


Fig. 3.4: Formation of three vortices<sup>[4]</sup>

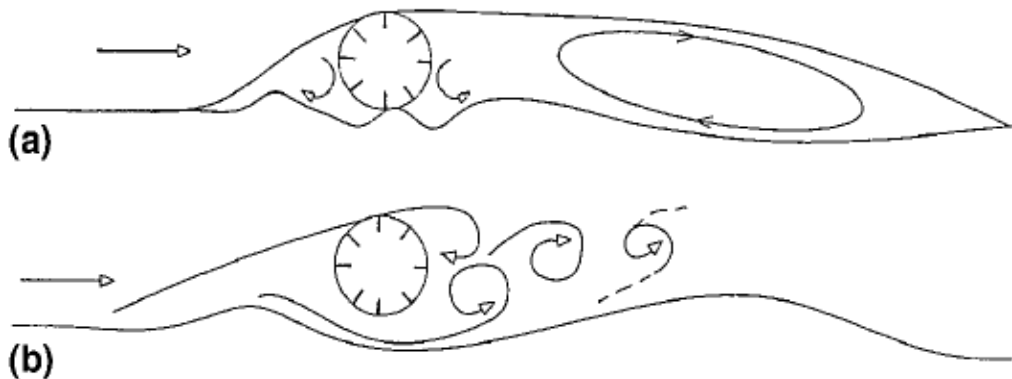


Fig. 3.5: Onset of scour process<sup>[8]</sup>

After the scour hole develops, vortex shedding takes place behind the pipe (Fig. 3.5 (b)). The scour hole has a gentle downstream slope, which allows almost symmetrical vortex shedding when the scour process reaches its equilibrium stage <sup>[6]</sup>. This downstream flow erodes the bed more heavily than does the upstream flow for two reasons: (1) the higher level of turbulence; and (2) the instantaneous velocity in the downstream vortices exceeding the undisturbed flow velocity by a factor of 2 or more. As a result of this increased erosion, the downstream slope becomes more gentle and the scour profile is characterized by an asymmetric shape <sup>[7]</sup>.

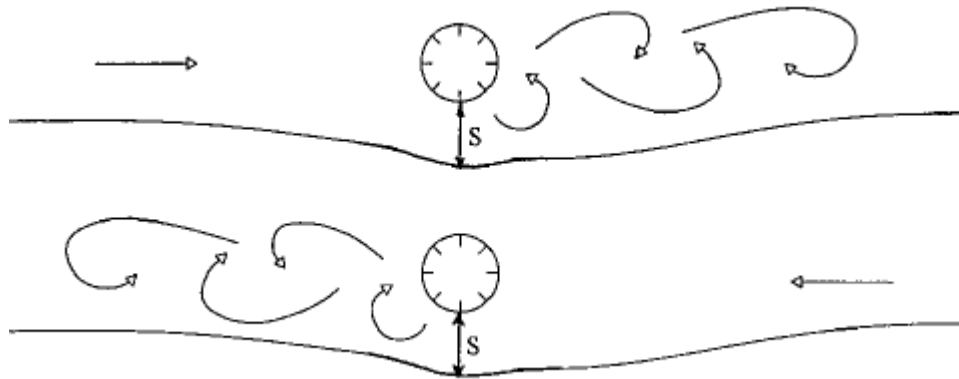


Fig. 3.6: Scour hole under the waves <sup>[8]</sup>

When the flow direction is oscillatory, a downstream formed wake system occurs on both sides of the pipeline. Lee wake erosion, which gives a gentle downstream slope, occurs on both sides of the pipe, as shown in Fig. 3.6. The different types of erosion occurring at the seabed are explained later in detail.

#### 3.4.1 Mechanism of onset of scour: Seepage flow and piping underneath the pipe

When a pipeline is laid on a sediment bed, and is subjected to a current, the pressure difference between the upstream and the downstream of the pipe will induce a seepage flow in the sand bed underneath the pipe, as shown in Fig. 3.7. When the current velocity is increased, a critical point is reached where the discharge of the seepage flow will be increased more rapidly than the driving pressure difference dictates, and simultaneously the surface of the sand at the immediate downstream of the pipe will rise, and eventually

a mixture of sand and water will break through the space underneath the pipe. This process is called as piping.

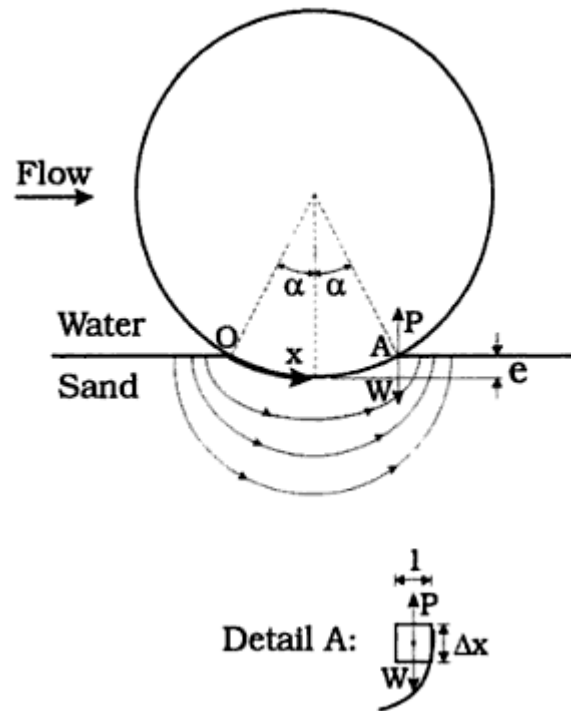


Fig. 3.7: Seepage flow underneath the pipe <sup>[3]</sup>

Consider the critical condition for the piping to occur for a cohesion-less granular material. There are basically two forces: one is the agitating force (i.e., the seepage force) and the other is the resisting force (i.e., the submerged weight of sand). The seepage force at the point where the sand-water mixture is expelled from the bed is directed vertically upwards (considering the bed as the potential line), and can be written as:

$$P = \frac{\partial p}{\partial x} \Delta x \quad (4)$$

In which  $p$  is the pressure;  $x$  is the distance along the perimeter of the pipe, measured from the junction between the upstream side of the pipe and the bed.  $\partial p / \partial x$  is the pressure gradient driving the seepage flow, and  $P$  is the force on a small element of sand

(of the size  $\Delta x \times 1 \times 1$ ) at the point where the mixture of sand and water breaks through. The submerged weight of the sand,  $W$ , is given by:

$$W = (\gamma_s - \gamma) \Delta x (1 - n) = \gamma (s - 1) (1 - n) \Delta x \quad (5)$$

Where  $s = \gamma_s / \gamma$  is the specific gravity of sand grains.  $\gamma$  is the specific weight of water, while  $\gamma_s$  is the specific weight of the sand grains, and  $n$  is the porosity. The critical condition will then occur when the seepage force  $P$  exceeds the submerged weight  $W$ :

$$P \geq W \quad (6)$$

Thus, from eq. 4, 5 and 6, the critical condition can be expressed by the following equation:

$$\frac{\partial}{\partial x} \left( \frac{p}{\gamma} \right) \geq (s - 1)(1 - n) \quad (7)$$

i.e., the critical condition occurs when the pressure gradient exceeds the flotation gradient.

#### Current Case:

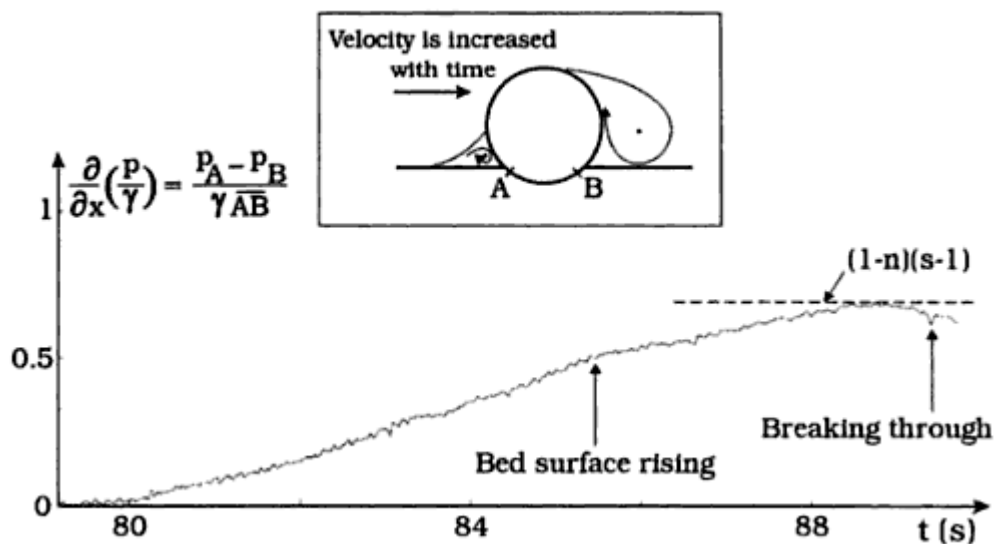


Fig. 3.8: Time series of pressure gradient underneath the pipe: Current case<sup>[3]</sup>

Fig. 3.8 shows the time series of the pressure gradient in the case of steady current <sup>[3]</sup>. In this test, the flow velocity was increased gradually until the critical point was reached. Following were the observations made:

1. With increasing velocity, the pressure gradient is increased.
2. As the pressure gradient increased, a point was reached where the surface of the sand at the immediate downstream of the pipe began to rise.
3. This stage continued for some period of time (about 5s [Fig. 3.8]), and was subsequently followed by the process where a mixture of sand and water breaks through (Fig. 3.9). The instant when the surface downstream starts the rise marks the instant when the pressure gradient exceeds the flotation gradient. Subsequently, grains were progressively removed and a breakthrough developed. The process depends on the porosity, internal friction and length of the flow path (longer the path, longer is the time taken for the breakthrough to develop).
4. The onset of scour never occurred concurrently along the length of the pipe in a two-dimensional fashion, but rather occurred locally, in a three-dimensional fashion.
5. The slight variation between the pressure gradient and the flotation gradient values from one test to the other, characterized by the standard deviation  $\sigma = 0.14$ , was attributed to the turbulent wake behind the pipeline.

It should be noted that the visual observations made in Sumer et al.'s work showed that, contrary to the generally accepted view <sup>[2, 8, 9]</sup>, the vortices generated at the downstream and upstream parts of the pipe did not undermine the pipe prior to the onset of scour, which would otherwise lead to a slight reduction in the length of the streamline of the seepage flow, presumably resulting in larger pressure-gradient forces.

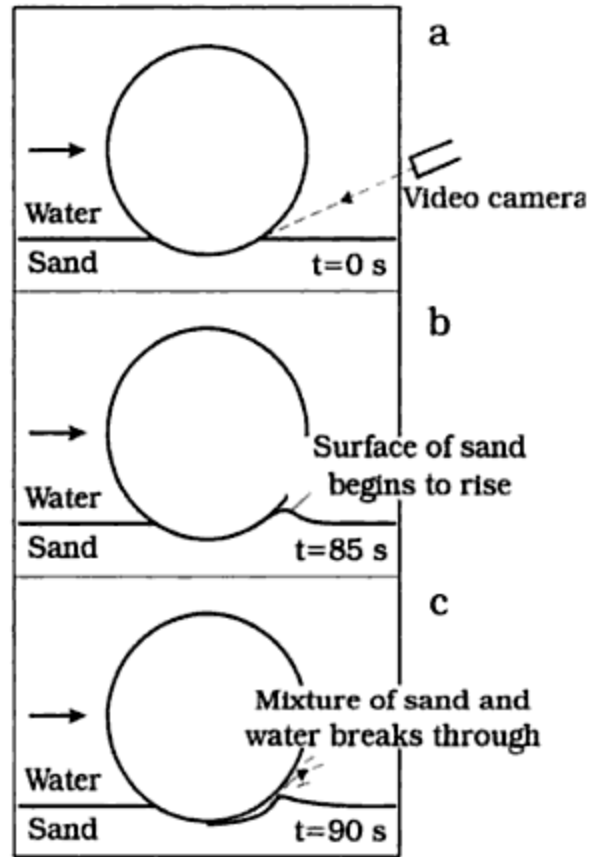


Fig. 3.9: Piping times corresponding to Fig. 3.8 <sup>[3]</sup>

**Wave Case:**

Fig. 3.10 shows the time series of the pressure gradient obtained in the experiments of Sumer et al. (2001) in the case of waves <sup>[3]</sup>. In these experiments, the wave height is increased gradually until the critical point is reached. The crests in the time series correspond to the crest half periods in the surface elevation, while the troughs correspond to the trough half periods. As seen, the onset of scour takes place in the crest half period. The pressure gradient in the trough half period is not large enough to cause piping.

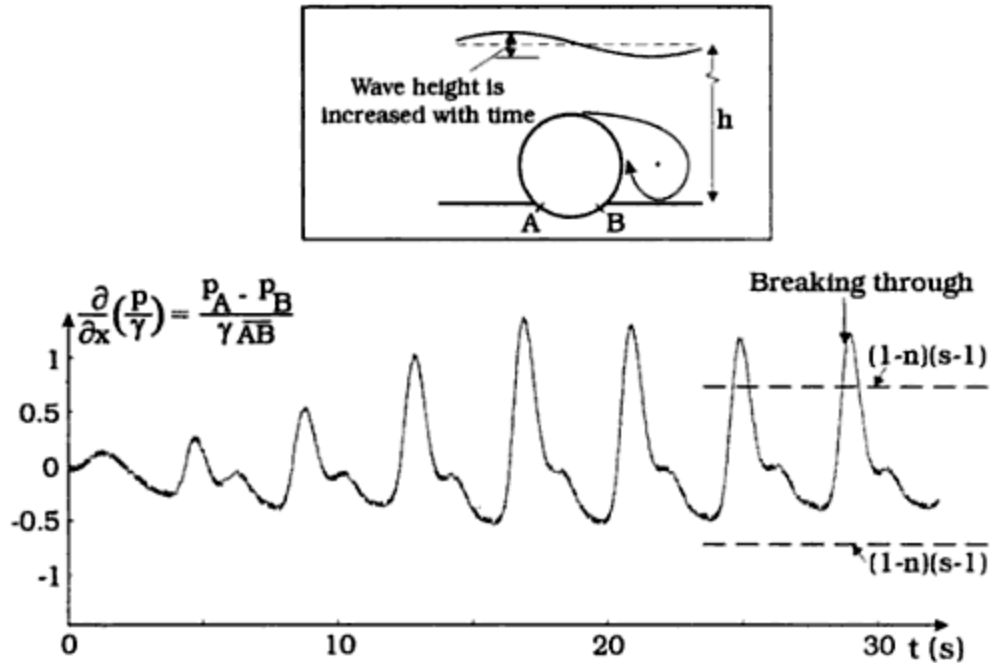


Fig. 3.10: Time series of pressure gradient underneath the pipe: Wave case <sup>[3]</sup>

As seen from the fig, the onset of scour occurs when the pressure gradient reaches the value  $(s - 1)(1 - n)$ , or even exceeds it. This results in somewhat different from that obtained for the current case (Fig. 3.8). This difference may be attributed to the time over which the sand is exposed to the critical pressure-gradient force. In the case of the current, this period is quite long, namely in the order of magnitude of 5 s, the mixture of sand and water breaks through only after 5 s. upon the application of the critical pressure gradient force. By contrast, in the case of waves, the pressure gradient necessary for the onset of scour is available only for a short period of time for each crest half period. Apparently this small exposure to the critical pressure gradient is not long enough for the piping to occur. It is only when the pressure gradient is increased further, and after some numbers of exposures that the piping takes place, resulting in the onset of scour. It may be added that the breakthrough is a progressive process; each wave loosens some grains on the exit side.

Sumer et al. (2001) noted that simultaneous measurements of the surface elevation ( $\eta$ ) and the pressure gradient indicate that there is a phase difference between them. The

pressure gradient (Fig. 3.10) lags about 20-25° behind the surface elevation. Fig 2.6 shows a sequence of flow pictures over one wave period. Sumer et al. pointed out that the moment where the onset of scour occurs coincides almost with the passage of the wave crest where the flow is in the direction of wave propagation, and the lee-wake (with Vortex M) is well established. This observation is consistent with the flow pattern in the case of the steady current.

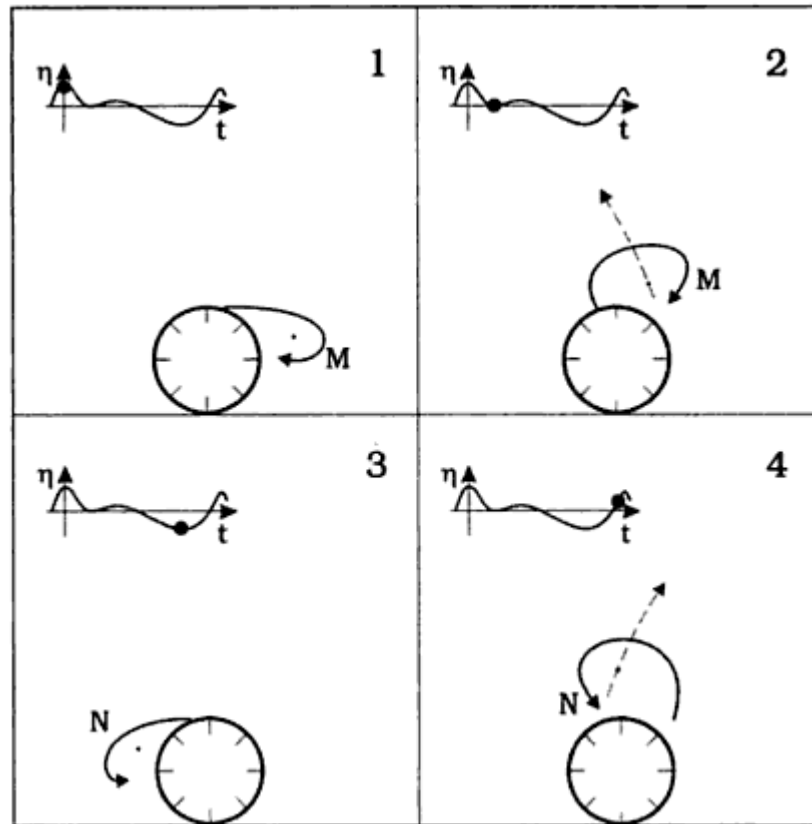


Fig. 3.11: Sequence of flow pictures over one wave cycle <sup>[3]</sup>

### 3.4.2 Parameters affecting the onset of scour process

Lucassen (1984) gave a brief description of the parameters affecting the onset of scour process for a submarine pipeline <sup>[10]</sup>. There parameters can be divided into three groups:

- a) The parameters which determine the flow pattern around the pipeline: The bed material underneath a pipeline can be eroded when the critical shear stress of the material is exceeded. The shear stress near the bottom is primarily determined by the flow velocity near the bottom which is a combination of the current velocity  $U$

and the orbital velocity  $U_*$ . The current velocity near the bottom is dependent on the bottom roughness  $r$ . The orbital velocity near the bottom is dependent on the wave characteristics  $H$  and  $T$  and the water depth  $h$ . Combining all this, we find the following relevant parameters which determine the flow pattern near the bottom (Fig. 3.11):

- U: Current velocity
- r: Bottom roughness
- H: Wave height
- T: Wave period
- h: Water depth
- $U_*$ : Orbital velocity

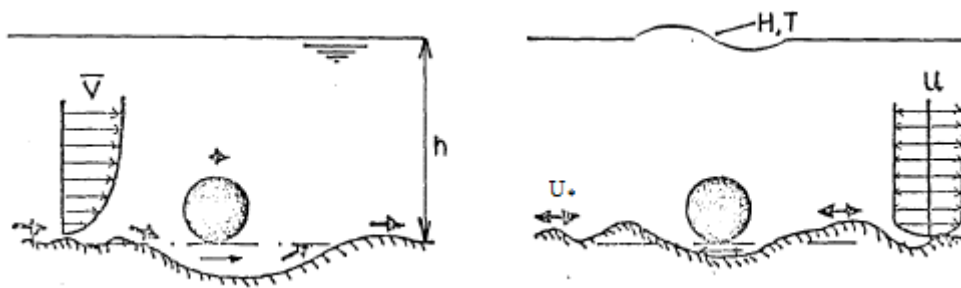


Fig. 3.12: The parameters which describe the flow pattern around the pipe <sup>[10]</sup>

- b) The parameters which describe the characteristics of the pipe: The flow pattern near the bottom is obstructed when a pipeline is laid on it. The change in the flow pattern is determined by the pipe characteristics and its location relative to the natural sea bottom. Assuming a cylindrical cross section, the dimensions of the pipe can be given by its diameter  $D$ . The roughness of the pipe is given by the roughness of the concrete coating, although organisms which may grow on the pipeline will vary the roughness considerably.

When a pipeline is laid in soft soil areas, the pipeline may sink a little into the bottom and in areas with mega ripples free spans may occur. The angles  $\theta_w$  and  $\theta_c$  indicate the direction of the predominant wave propagation and of the

predominant (tidal) current relative to the pipeline axis. Thus, the parameters describing the characteristics of the pipe are (Fig. 3.12):

D: Pipe diameter

r: Pipe roughness

e: Initial gap between the pipeline and the seabed

$\theta_w$ : Angle between pipe direction and predominant wave propagation

$\theta_c$ : Angle between pipe direction and predominant (tidal) current propagation

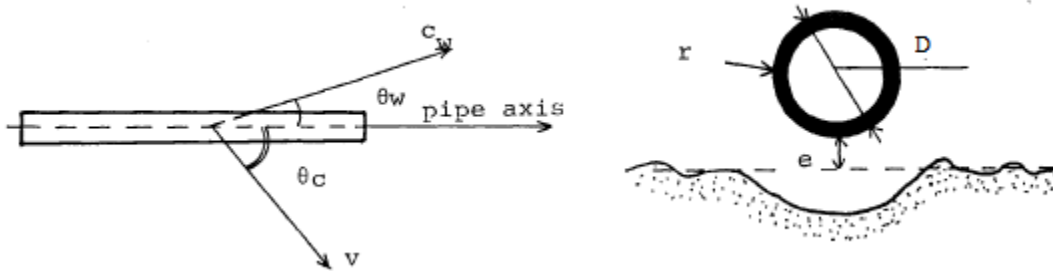


Fig. 3.12: The parameters which describe the characteristics of the pipe <sup>[10]</sup>

- c) The parameters which describe the characteristics of the seabed material: Whether the bottom will react on the change of the flow pattern due to the obstruction by the pipeline will depend on the characteristics of the bottom material. For a sandy bottom, this can be locally described by its mean grain diameter,  $d_{50}$ . Another parameter which depends on the seabed material characteristics is the undisturbed bed shear velocity  $U_f$  (which is used for describing Shield's parameter).

Combining the three types of parameters, we can come to the following relation:

$$\text{Scour process} = f(U, r, H, T, h, D, e, \theta_w, \theta_c, d_{50}, t) \quad (8)$$

In this relation, the time parameter  $t$  is added because some parameters such as  $U$ ,  $H$  and  $T$  will not be constant in time. Parameters which describe characteristics of the sea water such as the dynamic viscosity  $\mu$  and density  $\rho_w$ , or the bottom material density  $\rho_s$  are assumed to be constant. Together with the acceleration of gravity  $g$  they may be used to create dimensionless parameters.

If the bottom around the pipeline erodes, a scour hole can develop underneath the pipeline. If the pipe is stable, which will be the case for short spans and mild flow conditions, in due time the scour hole will develop towards a configuration as shown in Fig. 3.13. A two-dimensional scour hole can be described with the following parameters:

S: Maximum depth of the scour hole

P: Depth of scour hole underneath the pipe

$L_v$ : Horizontal distance from vertical pipe axis to sea bottom upstream of the pipe (or against the direction of wave propagation)

$L_a$ : Horizontal distance from vertical pipe axis to sea bottom downstream of the pipe (or in the direction of wave propagation)

A: total amount of eroded sediment

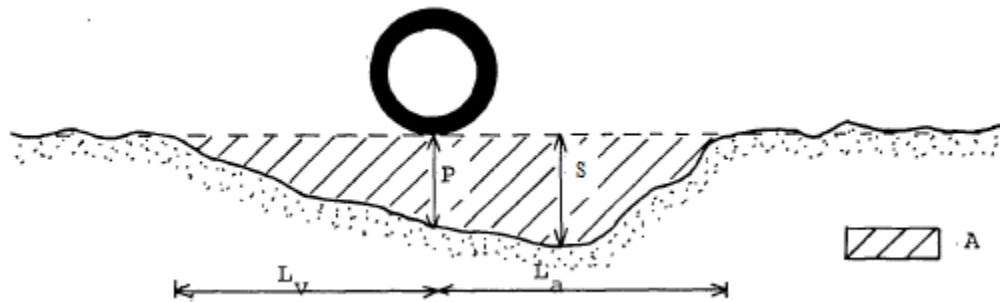


Fig. 3.13: Parameters of the scour hole <sup>[10]</sup>

Because the main interest lies in finding the maximum depth of the scour hole,  $S$  and whether the pipe will bury itself, and if so, how deep, the scour hole parameter  $e$  (or the dimensionless ratio of maximum scour depth to the pipeline diameter,  $e/D$ ) is considered to be the most important to investigate by researchers. Since the problem has been regarded only in a two-dimensional way having the pipe perpendicular to the current direction and wave propagation, the parameters  $\theta_w$  and  $\theta_c$  can be abandoned, which leads to:

$$S = f(U, r, H, T, h, D, e, d_{50}, t) \quad (9)$$

For prototype conditions it can be expected that the pipe will not be stable when spans grow and scour holes deepen. The pipeline may bend and touch the bottom. Because it is very difficult to scale the bending process, experiments are usually carried out with no initial gap between pipeline and seabed (i.e.,  $e = 0$ ). Also, Lucassen found after experiments with similar pipe diameter but different pipe roughness that the pipe roughness did not affect the value of the equilibrium scour hole depth. These limitations leave us with the following relation:

$$S = f(U, r, H, T, h, D, d_{50}) \quad (10)$$

Most of the researchers have followed this relation while predicting the equilibrium scour depth experimentally and while providing an empirical equation for calculating the same.

#### 3.4.3 Criterion for the onset of scour

##### **In steady current:**

The criterion for the onset of scour (eq. 7) can be written in the following non-dimensional form. Onset of scour occurs if:

$$[(\partial p^* / \partial x^*) \left( \frac{U^2}{gD(1-n)(s-1)} \right) + R]_{cr} \geq 1 \quad (11)$$

In which

$$p^* = \frac{p}{\rho U^2}, \quad x^* = \frac{x}{D} \quad (12)$$

$\rho$  is the water density,  $U$  is the undisturbed flow velocity at the top of the pipeline (the top velocity rather than the center-line velocity is adopted here, considering the cases where the pipeline may be buried with  $e/D$  larger than 0.5,  $e$  being the burial depth Fig. 3.7), and  $g$  is the acceleration due to gravity. The term  $R$  is a small, non-dimensional term, and is included here to represent the effects other than the pressure gradient force (mainly the effect of the vortices forming in front of the pipe and in the lee wake). Both  $\partial p^* / \partial x^*$  and

$R$  are essentially a function of the burial depth-to-diameter ratio,  $e/D$ . Therefore, the criterion for the onset of scour can be written in the following form:

$$\left[ \frac{U^2}{gD(1-n)(s-1)} \right] \geq f \left( \frac{e}{D} \right) \quad (13)$$

The function  $f(e/D)$  is to be determined from experiments. It may be noted that  $f$  is actually a function of not only  $e/D$ , but also the pipe Reynolds number,  $Re = UD/\nu$ , and the relative roughness  $k_s/D$  in which  $\nu$  is the kinematic viscosity and  $k_s$  is the surface roughness of the pipe. However, it is expected that the influence of these latter parameters will not be very significant, if there is no significant change in the flow regime, i.e., if the flow around the pipe does not change from the subcritical regime to the supercritical regime or from the supercritical regime to the trans-critical regime<sup>[11]</sup>.

#### **In waves:**

In the case of waves, the criterion given in Eq. 13 can be adopted provided that:

1.  $U$  is replaced by  $U_m$ , the maximum value of the orbital velocity of water particles at the bed, and
2. There will be an additional parameter regarding the function  $f$ , which is the Keulegan-Carpenter number.

The Keulegan-Carpenter number or KC number is defined as:

$$KC = U_m T_w / D \quad (14)$$

In which  $T_w$  = the wave period. If the orbital velocity is assumed to vary sinusoidally, KC can be written as:

$$KC = 2 \pi a / D \quad (15)$$

Where  $a$  = the amplitude of the orbital motion of the water particles at the bed, i.e.,

$a = U_m T_w / (2 \pi)$ . So the critical condition will be:

$$\left[ \frac{U^2}{gD(1-n)(s-1)} \right] \geq f \left( \frac{e}{D}, KC \right) \quad (16)$$

### 3.5 Tunnel Erosion

The onset of scour is followed by the stage called **tunnel erosion**.

In this initial stage, the gap between the pipe and the bed,  $e$ , remains small, i.e.,  $e \ll D$ , where  $D$  is the pipe diameter. During this stage, a substantial amount of water is diverted into the gap, as shown in Fig. 3.14, leading to very large velocities in the gap and presumably resulting in very large shear stresses on the bed just below the pipeline.

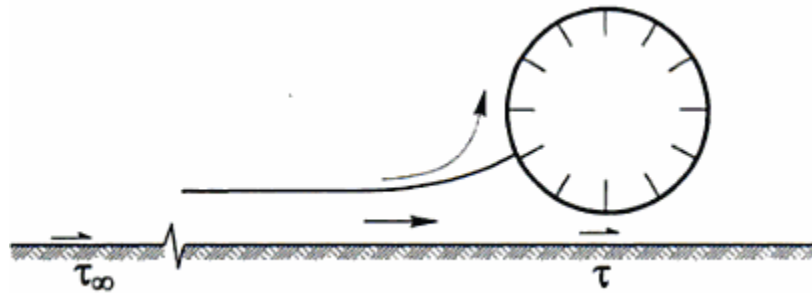


Fig. 3.14: Definition sketch of approach flow

The large increase in the bed shear stress below the pipe results in a tremendous increase in the sediment transport. In other words, Tunnel erosion underneath the pipe is a direct consequence of the increasing velocities underneath the pipe relative to the velocities at a comparable height above the undisturbed seabed upstream. Within the relatively short distance of the length of the scour hole in the direct vicinity of the pipe, the boundary layer over the seabed cannot adapt to the increasing velocities underneath the pipe<sup>[12, 13]</sup>. The result is an even higher bottom shear stress underneath the pipe than would be predicted from the increased current alone and a resultant greater transport capacity. This suggests that, immediately after the onset of scour, the scour under the pipeline will occur very violently; a mixture of sand and water flows in the form of a violent “jet” as seen in Fig. 3.15.

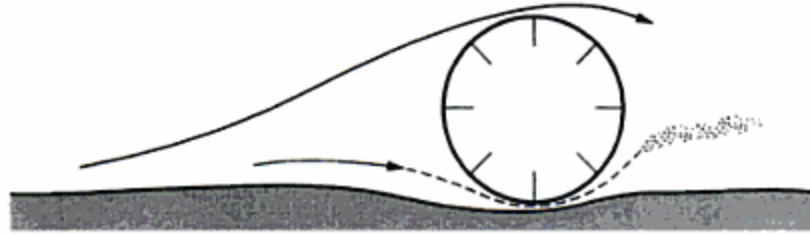


Fig. 3.15: Tunnel erosion below a pipeline

The tunnel erosion is “relieved” by the decrease of the gap-flow velocity, as the gap becomes larger and larger due to the scour. This stage is followed by the stage called the lee-wake erosion, which is described in the following section.

### 3.6 Lee-wake Erosion

In case of the two-dimensional scour below the pipeline, the previously described tunnel erosion is followed by the stage called the lee-wake erosion. Fig. 3.16 presents the results of a typical scour test where the pipe is rigidly fixed with initially a zero gap, and exposed to a steady current. The figure illustrates how the scour process evolves with time. The dotted line in the figure represents the equilibrium scour profile attained.

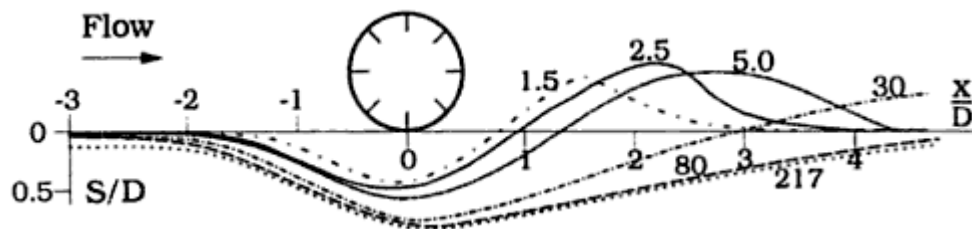


Fig. 3.16: Scour development: Current case (Time in minutes,  $\theta = 0.098$ )<sup>[2]</sup>

As seen, the scour occurs extremely fast at the beginning (tunnel erosion). As a result, a dune begins to form at the downstream side of the pipe. However, this dune gradually migrates downstream, and eventually may disappear as the scour progresses. Apparently, from the equilibrium profile in Fig. 3.16, there will be more scour at the downstream side of the pipe than at the upstream side of it, resulting presumably in a steep upstream slope and a more gentle downstream slope.



Fig. 3.17: Sediment motion caused by vortex passing overhead <sup>[7]</sup>

Basically, the scour at the stage of the lee-wake erosion is governed by the vortex shedding (Fig. 3.17), and the scour characteristics are controlled by the lee-wake of the pipe eventually <sup>[7]</sup>: When the gap between the pipeline and the bed reaches a certain value due to scour, the vortex shedding will begin to occur <sup>[7, 14]</sup>. The vortices shed from the bed side of the pipe sweep the bed, as they are convected downstream. The bed shear stress measurements show that the Shield's parameter can be easily raised by up to 4 times momentarily during these periods <sup>[3]</sup> indicating that the sediment transport at the lee side of the pipeline will increase tremendously due to this action. This will presumably result in the lee-wake erosion.

### 3.7 Equilibrium Scour Depth Stage

As mentioned earlier, the scour process finally reaches a steady state, the equilibrium stage (Fig. 3.16 dotted line profile). The equilibrium stage is reached when the bed shear stress along the bed underneath the pipe becomes constant and equal to its undisturbed value:

$$\tau = \tau_{\infty} \quad (17)$$

The first term also includes the effect of a large, local bed slope. Obviously, the sediment transport will be the same at all sections over the reach of the scour hole, and therefore the amount of sediment which enters the scour hole will be identical to that leaving the scour hole, when this stage is reached. This in turn implies that the scour process has stopped.

### 3.8 Research Work on Equilibrium Scour Depth

The scour depth develops towards the equilibrium stage through a transition period, as illustrated in Fig. 3.18 for a pipe rigidly placed on a bed with initially a zero gap. The depth corresponding to the fully-developed stage is called the equilibrium scour depth. Scour depth has been studied extensively by Chao and Hennesy (1972) <sup>[16]</sup>, Kjeldsen et al. (1973) <sup>[17]</sup>, Littlejohns (1977) <sup>[18]</sup>, Herbich (1981) <sup>[19]</sup>, Bijker and Leeuwenstein (1984) <sup>[20]</sup>, Lucassen (1984) <sup>[10]</sup>, Leeuwenstein et al. (1985) <sup>[21]</sup>, Ibrahim and Nalluri (1986) <sup>[22]</sup>, Mao (1986) <sup>[2]</sup>, Sumer and Fredsøe (1990) <sup>[14]</sup> etc.

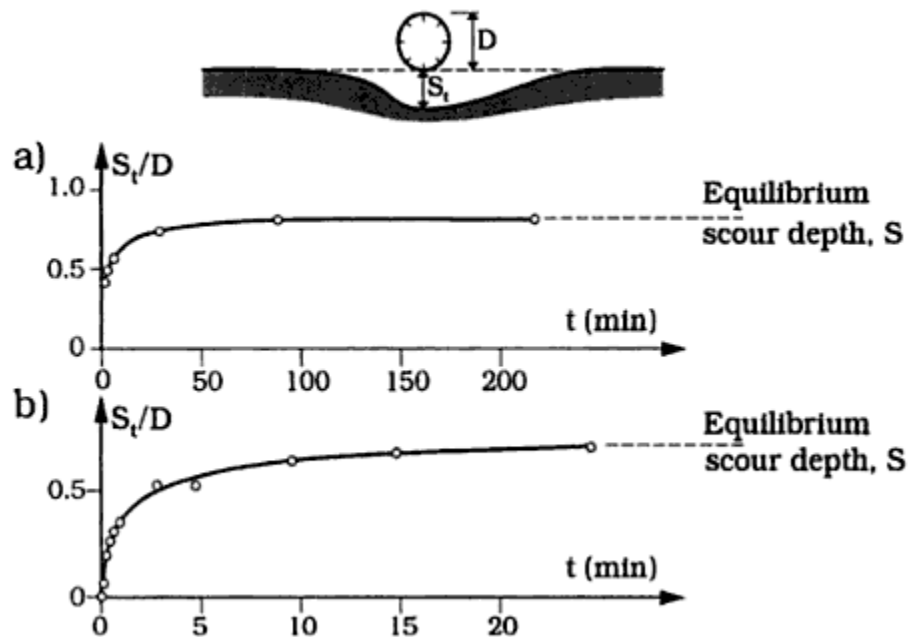


Fig. 3.18: Time development of scour depth

a) Current case,  $\theta = 0.098$  <sup>[2]</sup>, b) Wave case,  $\theta = 0.035$  <sup>[15]</sup>

Kjeldsen et al. (1973) were the first ones to establish an empirical relation between the equilibrium scour depth,  $S$ , the pipe diameter,  $D$ , and the flow velocity  $V$  as follows <sup>[17]</sup>:

$$S = 0.972 \left( \frac{V^2}{2g} \right)^{0.2} D^{0.8} \quad (18)$$

This is a dimensionally homogenous equation. The relation in the preceding equation suggests that the non-dimensional scour depth  $S/D$  is proportional to  $\theta^{0.2}$ :

$$\frac{S}{D} \propto \theta^{0.2} \quad (19)$$

In which  $\theta$  is the Shield's parameter defined by Eq. 3. The scour in Kjeldsen's study was for the live-bed situation ( $\theta > \theta_{cr}$ ) in which  $\theta_{cr}$  = the critical value of the Shield's parameter corresponding to the initiation of the motion at the bed.

Sumer et al. gave the following empirical equation relating the non-dimensional scour depth  $S/D$  with the Keulegan-Carpenter number for the case of live-bed <sup>[3]</sup>:

$$\frac{S}{D} = 0.1 \sqrt{KC} \quad (20)$$

Ibrahim and Nalluri (1986) proposed two equations based on an extensive experimental program on local scour around submarine pipeline conducted at the University of Newcastle upon Tyne <sup>[22]</sup>. The flume tests were conducted under the influence of unidirectional flow only. The empirical equations are:

$$\frac{S}{D} = 4.706 \left(\frac{U}{U^*}\right)^{0.89} \left(\frac{U}{\sqrt{gh}}\right)^{1.43} + 0.06 \quad (21)$$

$$\frac{S}{D} = 0.084 \left(\frac{U}{U^*}\right)^{-0.3} \left(\frac{U}{\sqrt{gh}}\right)^{-0.16} + 1.33 \quad (22)$$

Where  $S/D$  = non-dimensional scour depth,  $U$  = undisturbed mean flow velocity,  $U^*$  = critical velocity for sediment entrainment,  $g$  = acceleration due to gravity and  $h$  = flow depth.

Equations 21 and 22 apply to clear water and live-bed conditions respectively.

Etemad Shahidi et al. investigated scour around submarine pipelines to develop a relation between the wave-induced scour depth and the governing parameters <sup>[23]</sup>. Using machine

learning approaches such as Artificial Neural Networks (ANN), they developed the following equations for the live-bed condition:

$$\frac{S}{D} = 0.105 KC^{0.503} \exp\left(-0.284 \frac{e}{D}\right) \text{ for } e / D \leq 0.145 \quad (23)$$

$$\frac{S}{D} = 0.024 KC^{0.763} \exp\left(-0.631 \frac{e}{D}\right) \text{ for } e / D > 0.145 \quad (24)$$

Further simplification of the equations with the inclusion of the Shield's parameter gave the following equations for predicting the equilibrium scour depth:

$$\frac{S}{D} = 3.344 KC^{0.512} \theta^{1.296} \exp\left(-2.32 \frac{e}{D}\right) \text{ for } \theta \leq 0.064 \quad (25)$$

$$\frac{S}{D} = 0.149 KC^{0.477} \theta^{0.121} \exp\left(-0.472 \frac{e}{D}\right) \text{ for } \theta > 0.064 \text{ and } e / d \leq 0.145 \quad (26)$$

$$\frac{S}{D} = 0.048 KC^{0.782} \theta^{0.121} \exp\left(-0.942 \frac{e}{D}\right) \text{ for } \theta > 0.064 \text{ and } e / d > 0.145 \quad (27)$$

Eq. 24 is for the clear water case and eq. 26 and 27 are for the live-bed case. These formulae are consistent with the existing understanding of the relative importance of the parameters governing pipe scour depth. As discussed by Sumer and Fredsøe<sup>[3]</sup>, the main difference in live bed and clear water conditions is in the transport of the upstream sediments, which depends on  $\theta$ . The main splitting value is  $\theta = 0.064$ . This shows that the dataset is classified into two parts:  $\theta < 0.064$ , which is close to the clear water condition, and  $\theta > 0.064$ , which is close to the live bed condition. The critical Shield's parameter is calculated as follows:

$$\theta(\text{critical}) = \frac{0.24}{d^*} + 0.055 (1 - \exp(-0.02 d^*)) \quad (28)$$

Where  $d^*$  is the dimensionless diameter of the bed sand. The splitting value of the Shields parameter is close to the maximum value of the critical Shields parameter in Eq. 28. The

power of  $\theta$  is about 1.3 in Eq. 25. This shows that in the clear water condition,  $\theta$  is an important parameter and in this regime, the relationship between  $S/D$  and  $\theta$  is nearly linear. However, in the live bed condition ( $\theta > 0.064$ ) the power of  $\theta$  becomes more than ten times less (0.121); indicating that in the live bed condition the value of  $\theta$  is not as important as in the clear water condition.

Sumer and Fredsøe (2001) conducted wave flume and oscillatory U-Tube experiments to investigate scour around submarine pipelines. They proposed an empirical equation based on Lucassen's (1984) and their own experimental data <sup>[1]</sup>:

$$\frac{S}{D} = 0.1 \sqrt{KC} \exp\left(-0.6 \frac{e}{D}\right) \quad (29)$$

This equation is a development on the eq. 20 which considers the initial gap between the pipeline and the seabed.

Yasa R. predicted the wave induced scour depth using multiple regression analysis <sup>[24]</sup>. Several models were developed using different parameters and different combinations of them as input. Then the simplest and most accurate formulae were selected. Following are the formulae for live-bed and clear water conditions respectively:

$$\frac{S}{D} = 0.1 KC^{0.53} \exp\left(-1.54 \frac{e}{D}\right) \quad (30)$$

$$\frac{S}{D} = 0.07 KC^{0.59} \exp\left(-1.54 \frac{e}{D} + 1.02 \theta\right) \quad (31)$$

Using results from a series of model tests, including those conducted by Kjeldsen et al. (1973), Bijker and Leeuwenstein in 1984 proposed a slightly different empirical equation for computing scour depth at submarine pipelines <sup>[20]</sup>:

$$S = 0.929 \left( \frac{V}{2g} \right)^{0.26} \times D^{0.78} \times d_{50}^{-0.04} \quad (32)$$

Comparing Eq. 32 with that proposed by Kjeldsen et al. (Eq. 18), Bijker and Leeuwestein's equation includes a moderate effect of grain size on the scour depth. They also proposed a method for predicting prototype scour depth through a scale series. In other words, results obtained from model tests can be extrapolated and used to predict scour depth associated with a much larger pipe diameter and velocity. Verification of their method was done in the large-scale facilities at the Delft Hydraulics Laboratory and using a computational model. Their results showed that both Eqs. 18 and 32 underestimated the maximum scour depth.

One important conclusion drawn from Bijker and Leeuwestein's study is the inference that the scour depth under unidirectional current is always higher than that under pure wave action or the combined effect of wave and current with the same bottom shear stress.

Apart from investigating local scour at submarine pipelines per se, they also studied self-burial of submarine pipelines [21, 25]. They reported that pipelines can bury themselves down to three diameters under certain circumstances, and they proposed means to stimulate this process. Fins were attached to the pipelines with the intention of increasing the rate of scouring, thereby encouraging self-burial.

### **3.9 Scour Prevention and Repair**

Several methods have been tried in recent years, with varying success, to prevent or repair scour that has developed in and around submarine pipelines and offshore platforms. Some of these methods were designed for prevention while others were more for immediate repair of scour damage, in the hope that the repair would prevent future occurrence of scour. The methods can be grouped into the local and the global methods, and the active and the passive methods. The terms local and global, when used here to describe a scour repair method, refer to the size of the area being protected, rather than

the type of scour action, since global scour repair techniques will also affect areas of local scour. The active methods are distinguished from the passive, in that they involve a deliberate attempt to alter the flow characteristics to convert an area of sediment erosion to one of sediment deposition. The passive methods block or divert the water flow to prevent sediment erosion.

### **3.9.1 Local Methods**

The local methods of scour repair were generally the first to be attempted and some date back to the years when exploratory drilling was in progress. The local methods are not generally used today, since in the majority of instances, they did not provide a permanent cure for scour. The local methods tried and the dates of use are as follows:

1. Sandbags 1968 to 1986 (Passive): Bags, constructed of hessian or plastic, were filled with sand, shingle or gravel, and dumped into the sea from a suitable boat in an area near the scour. They were then arranged in place, in and around the scour hole, by divers.

The use of sandbags had several disadvantages. Large numbers were required to fill even a small scour hole. During the dumping operation, many of the bags were carried out of the immediate area of the job and were either lost or required additional diver time to relocate. Bundles of bags laid around the platform legs did little to change the flow characteristics and thus scour continued to occur around and underneath the bags. Regular maintenance was essential, requiring considerable expensive diving time.

2. Anti-Scour Device (ASD) 1968 to 1971 (Active) (Fig. 3.19): The ASD is a fine-mesh, nylon, circular net between 3 and 5 metres in diameter. A hole cut in the centre of the ASD allows it to be placed around the platform leg to be protected. It is clamped around the leg and stretched in tent-like fashion out from the leg and secured to the seabed by steel pins. The ASD net is designed to slow the water flow around the leg and thereby produce a zone of sediment deposition. The installation of the ASD is reasonably straightforward and could be accomplished

easily by divers. For a short period the device operated as designed and sediment did accumulate around the platform leg. In time, however, several of the nets suffered a large build-up of sand on top of the mesh and collapsed, while others lost one or more of the steel anchor pins and dangled uselessly from the leg. The main disadvantages of ASDs are an inherent weakness in the material and the poor securing system. The net is not strong enough to withstand the harsh deep sea conditions and the smooth steel pins have little purchase in the soft seabed. Most of the nets were lost within a year of installation and their replacement involved considerable expense. The experience gained from using the nets over 3 years indicated, however, that individual leg nets, if properly designed and securely anchored to the seabed and structure, could provide an effective and economic form of scour protection.

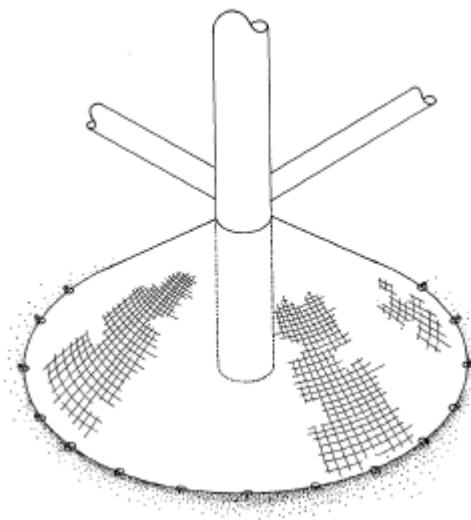


Fig. 3.19: Anti Scour Device (ASD) <sup>[26]</sup>

3. Sedimentary Deposition Device (SDD) 1971 to 1977 (Active) (Fig. 3.20): The SDD was originally developed in Denmark for use in protecting beaches from erosion. It was constructed of a multi-sided sheet of polypropylene perforated with a pattern of 100 mm diameter holes. The SDD was wrapped around the platform legs and the ends were bound together. The center was attached to the leg by an adjustable clamp that could be used to raise the SDD once total build-up of sand under the device had been achieved. Adjustable guy ropes were attached

to the corners of the sheet and were pinned to the seabed by auger-shaped anchors. The SDD was designed to prevent the agitation of the seabed around the leg by the downward components of flow, and also to decrease the flow velocity and thereby produce an area of sediment deposition. They were more robust than the ASDs which they replaced and were successful in preventing seabed scour around the platform legs. By 1977, the SDD sheets were used to cover areas of pipeline suspensions.

The major drawback of the SDD is its high maintenance cost. The amount of diving time required to inspect, repair and replace the large number of SDDs in service is extensive and costly. Removal of an old SDD and replacement with a new one requires up to nine dives since, due to the high tidal current velocity in the deep sea environment, diving may only take place during slack tide. Each device is inspected at a minimum frequency of twice per year, as experience showed that many required maintenance at this interval. At today's diving costs, the annual inspection and maintenance for the SDDs would amount to approximately \$2 million.

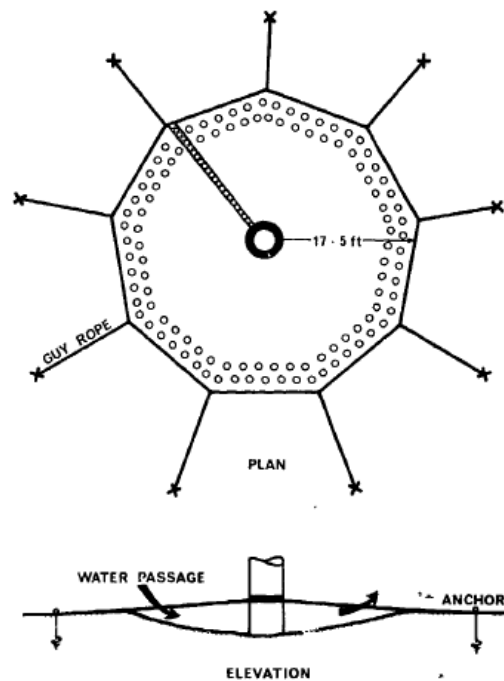


Fig. 3.20: Sedimentary Deposition Device (SDD) <sup>[27]</sup>

4. Glass Fibre Dome (GFD) 1974 to 1975 (Passive) (Fig. 3.21): The GFD is constructed of two glass fibre sections with a raised flange drilled to permit bolting of the two sections together. The dome is lowered in half-sections to the seafloor and bolted around the platform leg. The perimeter is pinned to the seafloor using the pin anchors developed for the SDD. The dome is then filled with sand through a small hatch in the top of the dome, using compressed air-driven pump to pump sand from the outlying seabed. GFDs were installed on three platforms in 1974 and their performance was monitored through 1975. The disadvantage of GFD is that they become detached from the submarine structures over time, and their replacement costs are high. They are prone to secondary scour similar to that experienced with the sandbags and thus afforded little active protection.

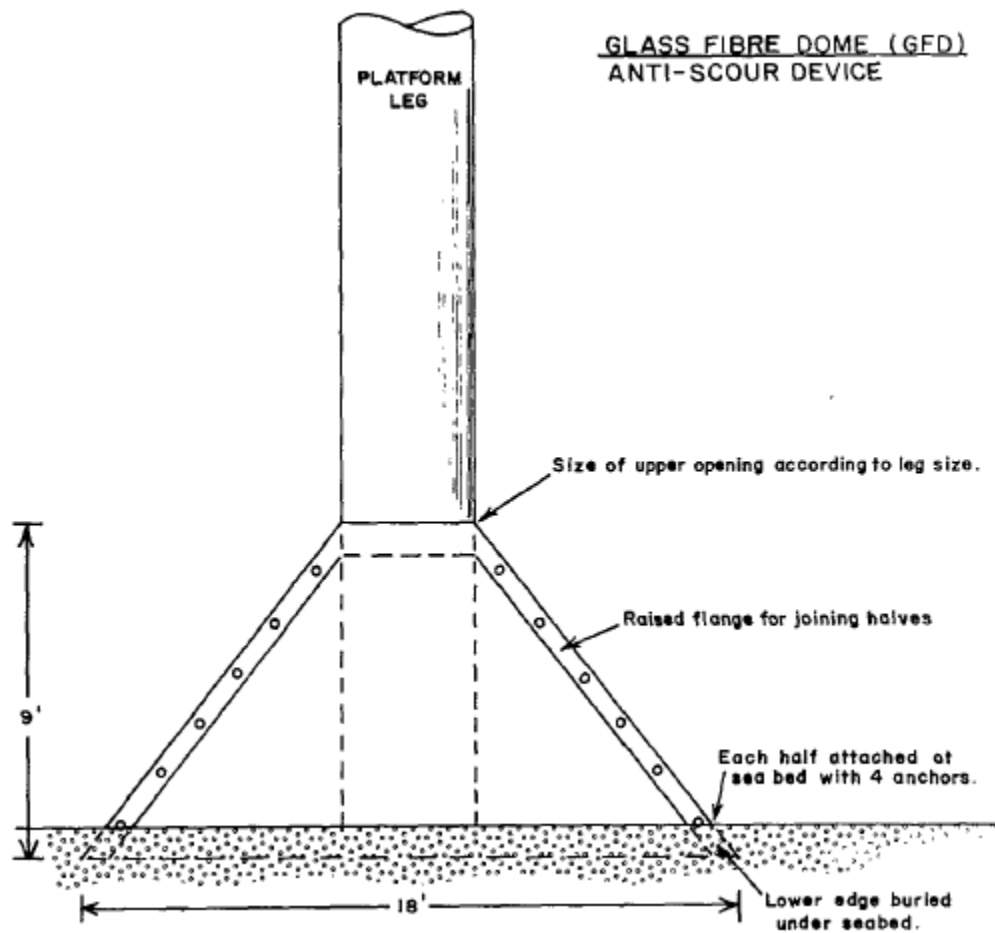


Fig. 3.21: Glass Fibre Dome (GFD) <sup>[26]</sup>

### 3.9.2 Global Methods

The global scour protection measures are apparently the only effective means of overcoming the problem of extensive scour. The local protection techniques described above may be successful in stopping the formation of scour holes under pipeline suspensions, but they do little to reduce the rate of global scour. The commonly used global scour protection methods are:

1. Artificial Seaweed 1970 to 1971 (Active): The artificial seaweed method is comprised of a framework of nylon rope with a one metre square mesh to which a large number of fine, polyester strands are attached simulating the effect of seaweed. The rope framework is installed within the periphery of the pipeline suspensions by attaching the corners of the mesh to the pipeline at a point a few feet above the sea floor. The system is designed to enable the polyester strands to hang down from the rope framework to the seafloor as a curtain of fibres. This sets up an obstruction to the flow, causing the sand to be deposited within the boundaries of the platform. The disadvantages are that the artificial seaweed does little to prevent and may also encourage global scouring outside the periphery. The strong fibres created a serious hazard for diving work and the portion of the pipeline below the rope framework is definitely out of bounds to the divers. The installation is difficult, time-consuming and expensive.
2. Gravel Pads, 1971 to Present (Passive): The placement of gravel pads to repair and prevent scour at offshore platforms dates back to at least 1960, when it was used in the Gulf of Mexico <sup>[28]</sup>. A large volume of gravel-sized material which can be rock, steel slag, or other dense substances, is used to fill in the scoured area and raise the seabed profile up to, or above, its original level. The particle size distribution within the pad must be small enough that migration of seabed fines through the pad is prevented, and large enough that the tidal flow will not dislodge the gravel. It is also desirable for the gravel to have sufficient porosity

for water to flow through it, thus preventing the buildup of pressure differentials which could cause the pad to buckle.

There are three generally accepted methods of placing the gravel: the split hopper, the side dumper and by pipe or chute. Depending on the location of the scour hole, one or all of these methods may be acceptable.

Split hopper vessels have been used primarily to fill areas of pipeline suspension. The material is carried in a large hold in the mid-section of the vessel. Once positioned, the split hopper is opened and the full volume of gravel is dropped in a matter of seconds into the scour hole.

The side dumper can be used for both pipeline suspensions and platform scour. The side dumping vessels can carry from 950 to 2500 tonnes of gravel in a number of compartments in the mid-section of the vessel. The gravel is pushed in batches over the side of the vessel by hydraulic rams inside each compartment. During the operation the tidal current direction and velocity are monitored to ensure that the vessel is correctly positioned for accurate placement of the gravel. Gravel chutes may be used when highly accurate placement of the gravel is required.

## CHAPTER 4: EXPERIMENTAL FINDINGS

Sumer et al. in 2001 conducted an experimental study on the onset of scour below submarine pipelines and its self-burial under the action of waves <sup>[1]</sup>. Two sets of experiments were conducted: 1) The experiments related to the onset of scour; and 2) The experiments related to the sinking of pipeline at the span shoulders. The experiments were carried out for combined current and wave case.

The experiments were carried out in a flume, 0.6 m in width, 0.8 m in depth and 26.5 m in length. The water depth was maintained constant at 0.33 m. Monochromatic waves were produced by a piston-type wave generator. A 0.10 m deep sand section was established in the flume, 3 m long, protected at the ends by crushed stones, The offshore end of the sand section was 11 m away from the wave generator. The test section was halfway through the length of the sand section. The pipe was rigidly fixed to the two side walls of the flume. A wave absorber at the onshore side of the wave flume was used to minimize the reflection. The flow velocity was measured by a bi-directional micropropeller.

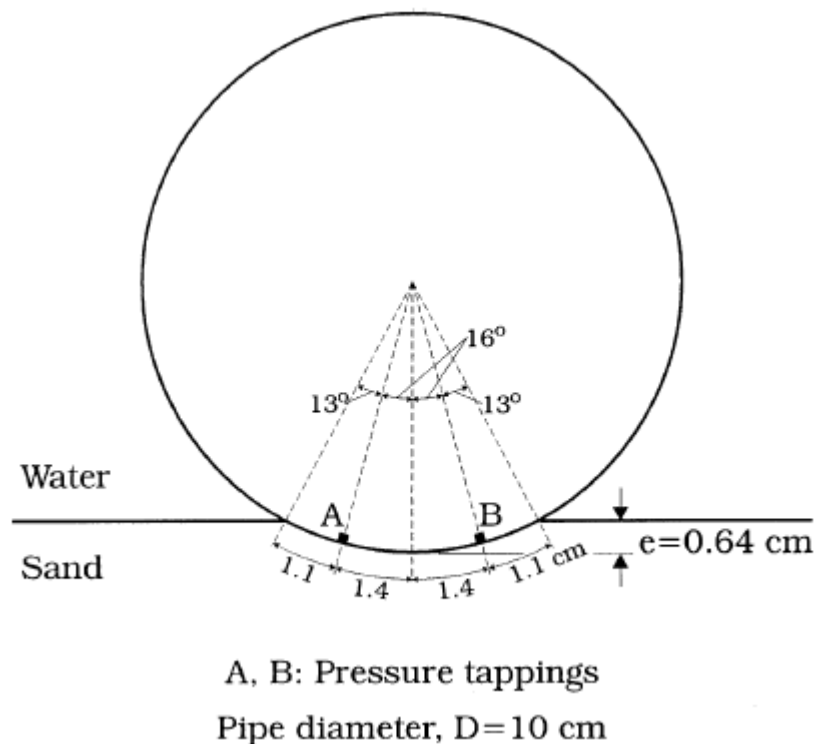


Fig. 4.1: Set up for the pressure measurement <sup>[1]</sup>

The pipe was equipped with two pressure tapings, 5 mm in diameter and covered with 40  $\mu\text{m}$  nylon filters, 32° apart, as shown in Fig. 4.1. The pressures were recorded automatically at a sampling frequency of 30 Hz. The length of recording was 30 s, corresponding to the length of the time from the start of the flow to the instant where the scouring commences. The purpose of the pressure measurement was to obtain the pressure gradient (that causes the seepage flow) at the instant of the onset of scour. In these measurements, the pipe was slightly buried with a burial depth of  $e = 0.64$  cm, as shown in Fig. 4.1.

The sand used in the experiments had a mean grain size  $d_{50} = 0.18$  mm. Flow visualization tests were also made. For this, a laser sheet of light scanned the experimental section and the flow was made visible with the sand itself.

The self-burial mechanism occurs as follows:

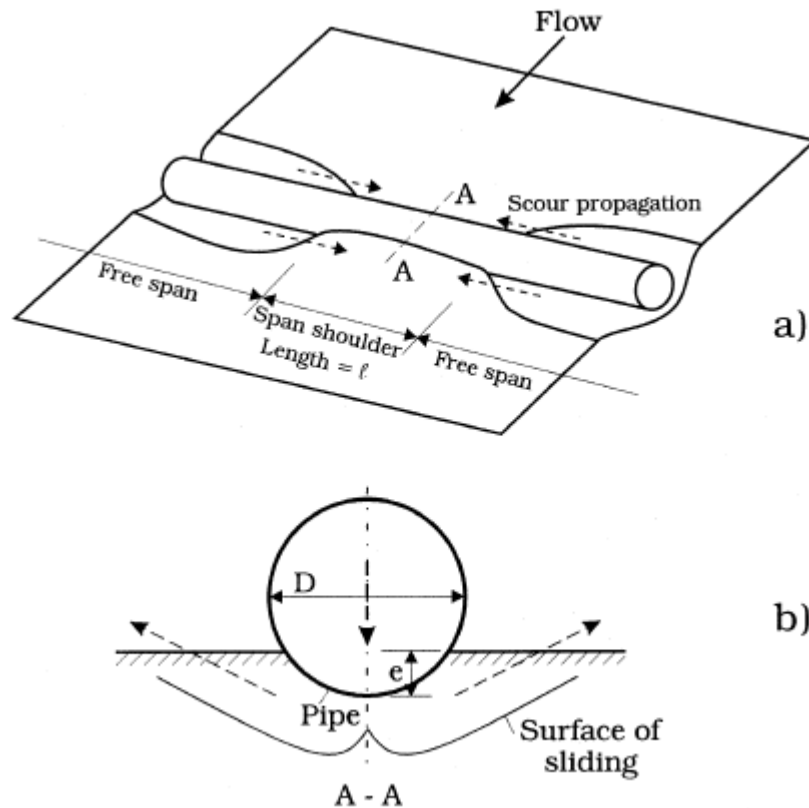


Fig. 4.2: Sinking of pipeline at span shoulder <sup>[1]</sup>

The scour begins to propagate along the length of the pipeline after the onset of the process <sup>[29]</sup>. As the process continues, the length of the free span will be larger and larger at the expense of the span shoulder. Therefore, more and more weight of the pipe will be exerted on the soil over a shorter and shorter length of the span shoulder (Fig. 4.2a). This process may reach such levels that the bearing capacity of the soil is exceeded, and therefore the soil fails. The failure occurs by sliding in the two outward directions, as indicated in Fig. 4.2b. This type of failure is known as a general shear failure in soil mechanics <sup>[30]</sup>. Clearly, as the scour continues, the bearing capacity of the soil will be exceeded constantly due to the continuous reduction of the bearing area, leading to the permanent sinking of the pipe. The process will stop only when the pipe sink to such depths that it will be protected against the scour. When the scour stops, obviously the constant failure of the soil will stop, and consequently the sinking of the pipe will come to an end.

As implied in the preceding paragraph, the scour at the two ends of the span shoulder (Fig. 4.2a) is the key mechanism for the process of pipe sinking. The scour process itself is governed mainly by the Keulegan–Carpenter number <sup>[31, 32]</sup>. This is essentially linked to the lee-wake, precisely in the same way as in the case of two-dimensional scour below a pipeline; the higher the Keulegan–Carpenter number, the longer the lee-wake that forms behind the pipe in each half period of the motion, the larger the scour <sup>[14]</sup>. This suggests that, first of all, the sinking depth (the self-burial depth),  $e$ , normalized by the pipe diameter  $D$ , should be a function of the Keulegan–Carpenter number  $KC$ ; and secondly  $e/D$  should increase with increasing  $KC$ . The findings of the experiment also suggest the same.

The findings of the experiments are as follows:

The experiments were carried out for two pipe diameters, 5cm and 10 cm. For both the cases, series of tests were carried out, and the average scour depth for each condition was found out. The sand grain size for both the conditions was  $d_{50} = 0.18$  mm. The wave height was 14.6 cm. The flow depth was 33 cm for both cases. The critical Shield's

parameter,  $\theta_{cr}$  was found to be 0.0352. Both the conditions were found to be live-bed conditions (as  $\theta > \theta_{cr}$  for both cases). The test conditions and the average equilibrium scour depth are given in the below table.

Table 1: Experimental findings for two cases: Case 1:  $D = 10$  cm, Case 2:  $D = 5$  cm

Sl. No.	Burial depth, $e/D$ (cm)	Pipe Diameter, $D$ (cm)	Wave Period, $T$ (s)	Current velocity, $U$ (cm/s)	Bed friction velocity, $U_*$ (cm/s)	Shield's parameter, $\theta$	Reynold's number, $Re$	KC number	Average Scour depth $S$ (cm)
1	0.07	10	1.8	12	1.5	0.08	$1.2 \times 10^4$	2.2	1.3
2	0.128	5	2.5	31.3	2.2	0.17	$1.6 \times 10^4$	16	2.0

Thus, it is seen that the average equilibrium scour depth increases with increase in  $KC$  number, and the burial depth  $e/D$  also increase with increase in  $KC$  number.

## CHAPTER 5: CALCULATIONS, RESULTS AND DISCUSSIONS

The main parameters which govern the equilibrium scour depth are the pipe diameter and the  $KC$  number. In order to see which empirical formula is the most accurate for predicting the scour depth, comparison is made with the experimental findings and the results obtained from each empirical formula discussed in the theoretical development section for different pipe diameters and  $KC$  numbers.

Case 1: For pipe diameter  $D = 10$  cm, the experimental findings were:

Table 2: Experimental findings for Case 1:  $D = 10$  cm

Sl. No.	Burial depth, $e/D$	Pipe Diameter, $D$ (cm)	Wave Period, $T$ (s)	Current velocity, $U$ (cm/s)	Bed friction velocity, $U_*$ (cm/s)	Shield's parameter, $\theta$	Reynold's number, $Re$	KC number	Average Scour depth (cm)
1	0.07	10	1.8	12	1.5	0.08	$1.2 \times 10^4$	2.2	1.3

Using the same data in the following equations:

According to Kjeldsen et al. (Eq. 18),

$$S = 0.972 \left( \frac{U^2}{2g} \right)^{0.2} D^{0.8}$$

i.e.,

$$S = 0.972 \left( \frac{(12 \times 10^{-2})^2}{2 \times 9.81} \right)^{0.2} \times 10^{0.8}$$

$$S = 1.448 \text{ cm}$$

According to Sumer et al. (Eq. 20),

$$\frac{S}{D} = 0.1 \sqrt{KC}$$

$$\frac{S}{10} = 0.1 \sqrt{2.2}$$

$$S = 1.483 \text{ cm}$$

According to Ibrahim and Nalluri (Eq. 22),

$$\frac{S}{D} = 0.084 \left( \frac{U}{U_*} \right)^{-0.3} \left( \frac{U}{\sqrt{gh}} \right)^{-0.16} + 1.33$$

$$\frac{S}{10} = 0.084 \times \left( \frac{12}{1.5} \right)^{-0.3} \times \left( \frac{12 \times 10^{-2}}{\sqrt{9.81 \times 33 \times 10^{-2}}} \right)^{-0.16} + 1.33$$

$$S = 1.39 \text{ cm}$$

According to Etemad-Shahidi et al. (Eq. 23),

$$\frac{S}{D} = 0.105 KC^{0.503} \exp\left(-0.284 \frac{e}{D}\right) \text{ for } e/D \leq 0.145$$

$$\frac{S}{10} = 0.105 \times 2.2^{0.503} \exp(-0.284 \times 0.07)$$

$$S = 1.547 \text{ cm}$$

According to Etemad-Shahidi et al. (Eq. 26),

$$\frac{S}{D} = 0.149 KC^{0.477} \theta^{0.121} \exp\left(-0.472 \frac{e}{D}\right) \text{ for } \theta > 0.064 \text{ and } e/d \leq 0.145$$

$$\frac{S}{10} = 0.149 \times 2.2^{0.477} \times 0.08^{0.121} \exp(-0.472 \times 0.07)$$

$$S = 1.39 \text{ cm}$$

According to Sumer and Fredsøe 2002 (Eq. 29),

$$\frac{S}{D} = 0.1 \sqrt{KC} \exp\left(-0.6 \frac{e}{D}\right)$$

$$\frac{S}{10} = 0.1 \sqrt{2.2} \exp(-0.6 \times 0.07)$$

$$S = 1.422 \text{ cm}$$

According to Yasa, R (Eq. 30),

$$\frac{S}{D} = 0.1 KC^{0.53} \exp\left(-1.54 \frac{e}{D}\right)$$

$$\frac{S}{10} = 0.1 \times 2.2^{0.53} \exp(-1.54 \times 0.07)$$

$$S = 1.364 \text{ cm}$$

According to Bijker and Leeuwestein (Eq. 32),

$$S = 0.929 \left(\frac{V}{2g}\right)^{0.26} \times D^{0.78} \times d_{50}^{-0.04}$$

$$S = 0.929 \left(\frac{12 \times 10^{-2}}{2 \times 9.81}\right)^{0.26} \times 10^{0.78} \times (0.18 \times 10^{-3})^{-0.04}$$

$$S = 1.2103 \text{ cm}$$

Case 2: For pipe diameter  $D = 5$  cm, the experimental findings were:

Table 3: Experimental findings for Case 2:  $D = 5$  cm

Sl. No.	Burial depth, $e/D$	Pipe Diameter, $D$ (cm)	Wave Period, $T$ (s)	Current velocity, $U$ (cm/s)	Bed friction velocity, $U_*$ (cm/s)	Shield's parameter, $\theta$	Reynold's number, $Re$	KC number	Average Scour depth (cm)
2	0.128	5	2.5	31.3	2.2	0.17	$1.6 \times 10^4$	16	2.0

Using the same data in the following equations:

According to Kjeldsen et al. (Eq. 18),

$$S = 0.972 \left(\frac{U^2}{2g}\right)^{0.2} D^{0.8}$$

i.e.,

$$S = 0.972 \left(\frac{(31.3 \times 10^{-2})^2}{2 \times 9.81}\right)^{0.2} \times 5^{0.8}$$

$$S = 1.22 \text{ cm}$$

According to Sumer et al. (Eq. 20),

$$\frac{S}{D} = 0.1 \sqrt{KC}$$

$$\frac{S}{5} = 0.1 \sqrt{16}$$

$$S = 2 \text{ cm}$$

According to Ibrahim and Nalluri (Eq. 22),

$$\frac{S}{D} = 0.084 \left( \frac{U}{U^*} \right)^{-0.3} \left( \frac{U}{\sqrt{gh}} \right)^{-0.16} + 1.33$$

$$\frac{S}{5} = 0.084 \times \left( \frac{31.3}{2.2} \right)^{-0.3} \times \left( \frac{31.3 \times 10^{-2}}{\sqrt{9.81 \times 33 \times 10^{-2}}} \right)^{-0.16} + 1.33$$

$$S = 1.38 \text{ cm}$$

According to Etemad-Shahidi et al. (Eq. 23),

$$\frac{S}{D} = 0.105 KC^{0.503} \exp\left(-0.284 \frac{e}{D}\right) \text{ for } e/D \leq 0.145$$

$$\frac{S}{5} = 0.105 \times 16^{0.503} \exp(-0.284 \times 0.128)$$

$$S = 2.042 \text{ cm}$$

According to Etemad-Shahidi et al. (Eq. 26),

$$\frac{S}{D} = 0.149 KC^{0.477} \theta^{0.121} \exp\left(-0.472 \frac{e}{D}\right) \text{ for } \theta > 0.064 \text{ and } e/d \leq 0.145$$

$$\frac{S}{5} = 0.149 \times 16^{0.477} \times 0.17^{0.121} \exp(-0.472 \times 0.128)$$

$$S = 2.124 \text{ cm}$$

According to Sumer and Fredsøe 2002 (Eq. 29),

$$\frac{S}{D} = 0.1 \sqrt{KC} \exp\left(-0.6 \frac{e}{D}\right)$$

$$\frac{S}{5} = 0.1 \sqrt{16} \exp(-0.6 \times 0.128)$$

$$S = 1.85 \text{ cm}$$

According to Yasa, R (Eq. 30),

$$\frac{S}{D} = 0.1 KC^{0.53} \exp\left(-1.54 \frac{e}{D}\right)$$

$$\frac{S}{5} = 0.1 \times 16^{0.53} \exp(-1.54 \times 0.128)$$

$$S = 1.785 \text{ cm}$$

According to Bijker and Leeuwestein (Eq. 32),

$$S = 0.929 \left(\frac{V}{2g}\right)^{0.26} \times D^{0.78} \times d_{50}^{-0.04}$$

$$S = 0.929 \left(\frac{31.3 \times 10^{-2}}{2 \times 9.81}\right)^{0.26} \times 5^{0.78} \times (0.18 \times 10^{-3})^{-0.04}$$

$$S = 1.57 \text{ cm}$$

Case 3: For pipe diameter  $D = 2$  cm, the experimental findings were:

Table 4: Experimental findings for Case 3:  $D = 2$  cm

Sl. No.	Burial depth, $e/D$	Pipe Diameter, $D$ (cm)	Wave Period, $T$ (s)	Current velocity, $U$ (cm/s)	Bed friction velocity, $U_*$ (cm/s)	Shield's parameter, $\theta$	Reynold's number, $Re$	KC number	Average Scour depth (cm)
2	0.2	2	3	8.2	2	0.11	$4.4 \times 10^4$	22	0.83

Using the same data in the following equations:

According to Kjeldsen et al. (Eq. 18),

$$S = 0.972 \left( \frac{U^2}{2g} \right)^{0.2} D^{0.8}$$

i.e.,

$$S = 0.972 \left( \frac{(8.2 \times 10^{-2})^2}{2 \times 9.81} \right)^{0.2} \times 2^{0.8}$$

$$S = 0.343 \text{ cm}$$

According to Sumer et al. (Eq. 20),

$$\frac{S}{D} = 0.1 \sqrt{KC}$$

$$\frac{S}{2} = 0.1 \sqrt{22}$$

$$S = 0.938 \text{ cm}$$

According to Ibrahim and Nalluri (Eq. 22),

$$\frac{S}{D} = 0.084 \left( \frac{U}{U^*} \right)^{-0.3} \left( \frac{U}{\sqrt{gh}} \right)^{-0.16} + 1.33$$

$$\frac{S}{2} = 0.084 \times \left( \frac{8.2}{2} \right)^{-0.3} \times \left( \frac{8.2 \times 10^{-2}}{\sqrt{9.81 \times 33 \times 10^{-2}}} \right)^{-0.16} + 1.33$$

$$S = 1.42 \text{ cm}$$

According to Etemad-Shahidi et al. (Eq. 23),

$$\frac{S}{D} = 0.105 KC^{0.503} \exp\left(-0.284 \frac{e}{D}\right) \text{ for } e/D \leq 0.145$$

$$\frac{S}{2} = 0.105 \times 22^{0.503} \exp(-0.284 \times 0.2)$$

$$S = 0.912 \text{ cm}$$

According to Etemad-Shahidi et al. (Eq. 26),

$$\frac{S}{D} = 0.149 KC^{0.477} \theta^{0.121} \exp\left(-0.472 \frac{e}{D}\right) \text{ for } \theta > 0.064 \text{ and } e/d \leq 0.145$$

$$\frac{S}{2} = 0.149 \times 22^{0.477} \times 0.11^{0.121} \exp(-0.472 \times 0.2)$$

$$S = 0.907 \text{ cm}$$

According to Sumer and Fredsøe 2002 (Eq. 29),

$$\frac{S}{D} = 0.1 \sqrt{KC} \exp\left(-0.6 \frac{e}{D}\right)$$

$$\frac{S}{2} = 0.1 \sqrt{22} \times \exp(-0.6 \times 0.2)$$

$$S = 0.832 \text{ cm}$$

According to Yasa, R (Eq. 30),

$$\frac{S}{D} = 0.1 KC^{0.53} \exp\left(-1.54 \frac{e}{D}\right)$$

$$\frac{S}{2} = 0.1 \times 22^{0.53} \exp(-1.54 \times 0.2)$$

$$S = 0.756 \text{ cm}$$

According to Bijker and Leeuwestein (Eq. 32),

$$S = 0.929 \left(\frac{V}{2g}\right)^{0.26} \times D^{0.78} \times d_{50}^{-0.04}$$

$$S = 0.929 \left(\frac{8.2 \times 10^{-2}}{2 \times 9.81}\right)^{0.26} \times 2^{0.78} \times (0.18 \times 10^{-3})^{-0.04}$$

$$S = 0.542 \text{ cm}$$

For all the three cases, the percentage error was calculated for each equation (Appendix I) and is tabulated below:

Table 5: Calculation of Average Error

Equation	Percentage Error = $\left(\frac{ Calculated\ value - Experimental\ value }{Experimental\ value}\right) \times 100$			Average % Error
	Case 1: $D = 10\text{ cm}$	Case 2: $D = 5\text{ cm}$	Case 3: $D = 2\text{ cm}$	
Kjeldsen et al.	11.38	39	58.67	36.35
Sumer et al.	14.08	0	13.01	9.03
Ibrahim and Nalluri	6.92	31	71	36.31
Etemad-Shahidi et al.	19	2.1	9.88	10.33
Etemad-Shahidi et al. (with Shield's parameter)	6.92	6.2	9.277	7.46
Sumer and Fredsøe	9.38	7.5	0.241	5.687
Yasa R	4.92	10.75	8.916	8.19
Bijker and Leeuwestein	6.9	21.5	34.7	21.03

From the above results, it is clear that the most accurate scour depth prediction calculations can be obtained from equation 23 (Etemad-Shahidi et al.), equation 26 (Etemad-Shahidi et al. (with Shield's parameter)), equation 29 (Sumer and Fredsøe) and equation 30 (Yasa R). The reason why other equations have such errors is due to the approximation of parameters made in these equations. Also, the empirical equations have been developed using experimental findings, and the experimental test conditions also play a part in the results obtained.

Now, in order to show that the equilibrium scour depth increases as the value of  $KC$  number increases, the equilibrium scour depth is calculated for the three diameter cases with different governing parameters. They are as follows:

**Case 1a:** For pipe diameter  $D = 10$  cm, assuming that the wave period and seabed characteristics remain constant, taking  $KC$  number = 8, we have,

$$KC = \frac{U \times T}{D}$$

$$8 = \frac{U \times 2}{10}$$

Therefore,

$$U = 40 \text{ cm/s}$$

Hence, the input parameters are:

Table 6: Input parameters for  $D = 10$  cm,  $KC = 8$

Sl. No.	Burial depth, $e/D$	Pipe Diameter, $D$ (cm)	Wave Period, $T$ (s)	Current velocity, $U$ (cm/s)	Bed friction velocity, $U_*$ (cm/s)	Shield's parameter, $\theta$	Reynold's number, $Re$	KC number
1	0.07	10	2	40	1.5	0.08	$1.2 \times 10^4$	8.0

Calculating the scour depth using equations 23, 26, 29 and 30 (since they are more accurate than the rest),

According to Etemad-Shahidi et al. (Eq. 23),

$$\frac{S}{D} = 0.105 KC^{0.503} \exp\left(-0.284 \frac{e}{D}\right) \text{ for } e/D \leq 0.145$$

$$\frac{S}{10} = 0.105 \times 8.0^{0.503} \exp(-0.284 \times 0.07)$$

$$S = 2.93 \text{ cm}$$

According to Etemad-Shahidi et al. (Eq. 26),

$$\frac{S}{D} = 0.149 KC^{0.477} \theta^{0.121} \exp\left(-0.472 \frac{e}{D}\right) \text{ for } \theta > 0.064 \text{ and } e / d \leq 0.145$$

$$\frac{S}{10} = 0.149 \times 8.0^{0.477} \times 0.08^{0.121} \exp(-0.472 \times 0.07)$$

$$S = 2.863 \text{ cm}$$

According to Sumer and Fredsøe 2002 (Eq. 29),

$$\frac{S}{D} = 0.1 \sqrt{KC} \exp\left(-0.6 \frac{e}{D}\right)$$

$$\frac{S}{10} = 0.1 \sqrt{8.0} \exp(-0.6 \times 0.07)$$

$$S = 2.712 \text{ cm}$$

According to Yasa, R (Eq. 30),

$$\frac{S}{D} = 0.1 KC^{0.53} \exp\left(-1.54 \frac{e}{D}\right)$$

$$\frac{S}{10} = 0.1 \times 8.0^{0.53} \exp(-1.54 \times 0.07)$$

$$S = 2.703 \text{ cm}$$

Since there is not a large difference between the results obtained, the equilibrium scour depth for the given input conditions can be predicted to be in the range of 2.7 – 2.8 cm.

**Case 1b:** For pipe diameter  $D = 10$  cm, assuming that the wave period and seabed characteristics remain constant, taking  $KC$  number = 16, we have,

$$KC = \frac{U \times T}{D}$$

$$16 = \frac{U \times 2}{10}$$

Therefore,

$$U = 80 \text{ cm/s}$$

Hence, the input parameters are:

Table 7: Input parameters for  $D = 10 \text{ cm}$ ,  $KC = 16$

Sl. No.	Burial depth, $e/D$	Pipe Diameter, $D$ (cm)	Wave Period, $T$ (s)	Current velocity, $U$ (cm/s)	Bed friction velocity, $U_*$ (cm/s)	Shield's parameter, $\theta$	Reynold's number, $Re$	KC number
1	0.07	10	2	80	1.5	0.08	$1.2 \times 10^4$	16

Calculating the scour depth using equations 23, 26, 29 and 30 (since they are more accurate than the rest),

According to Etemad-Shahidi et al. (Eq. 23),

$$\frac{S}{D} = 0.105 KC^{0.503} \exp\left(-0.284 \frac{e}{D}\right) \text{ for } e/D \leq 0.145$$

$$\frac{S}{10} = 0.105 \times 16^{0.503} \exp(-0.284 \times 0.07)$$

$$S = 4.152 \text{ cm}$$

According to Etemad-Shahidi et al. (Eq. 26),

$$\frac{S}{D} = 0.149 KC^{0.477} \theta^{0.121} \exp\left(-0.472 \frac{e}{D}\right) \text{ for } \theta > 0.064 \text{ and } e/d \leq 0.145$$

$$\frac{S}{10} = 0.149 \times 16^{0.477} \times 0.08^{0.121} \exp(-0.472 \times 0.07)$$

$$S = 3.985 \text{ cm}$$

According to Sumer and Fredsøe 2002 (Eq. 29),

$$\frac{S}{D} = 0.1 \sqrt{KC} \exp\left(-0.6 \frac{e}{D}\right)$$

$$\frac{S}{10} = 0.1 \sqrt{16} \times \exp(-0.6 \times 0.07)$$

$$S = 3.835 \text{ cm}$$

According to Yasa, R (Eq. 30),

$$\frac{S}{D} = 0.1 KC^{0.53} \exp\left(-1.54 \frac{e}{D}\right)$$

$$\frac{S}{10} = 0.1 \times 16^{0.53} \exp(-1.54 \times 0.07)$$

$$S = 3.903 \text{ cm}$$

Since there is not a large difference between the results obtained, the equilibrium scour depth for the given input conditions can be predicted to be in the range of 3.9 – 4.1 cm.

**Case 2a:** For pipe diameter  $D = 5$  cm, assuming that the wave period and seabed characteristics remain constant, taking  $KC$  number = 7, we have,

$$KC = \frac{U \times T}{D}$$

$$7 = \frac{U \times 2.5}{5}$$

Therefore,

$$U = 14 \text{ cm/s}$$

Hence, the input parameters are:

Table 8: Input parameters for  $D = 5$  cm,  $KC = 7$

Sl. No.	Burial depth, $e/D$	Pipe Diameter, $D$ (cm)	Wave Period, $T$ (s)	Current velocity, $U$ (cm/s)	Bed friction velocity, $U_*$ (cm/s)	Shield's parameter, $\theta$	Reynold's number, $Re$	KC number
1	0.128	5	2.5	14	2.2	0.17	$1.6 \times 10^4$	7

Calculating the scour depth using equations 23, 26, 29 and 30 (since they are more accurate than the rest),

According to Etemad-Shahidi et al. (Eq. 23),

$$\frac{S}{D} = 0.105 KC^{0.503} \exp\left(-0.284 \frac{e}{D}\right) \text{ for } e/D \leq 0.145$$

$$\frac{S}{5} = 0.105 \times 7^{0.503} \times \exp(-0.284 \times 0.128)$$

$$S = 1.347 \text{ cm}$$

According to Etemad-Shahidi et al. (Eq. 26),

$$\frac{S}{D} = 0.149 KC^{0.477} \theta^{0.121} \exp\left(-0.472 \frac{e}{D}\right) \text{ for } \theta > 0.064 \text{ and } e/d \leq 0.145$$

$$\frac{S}{5} = 0.149 \times 7^{0.477} \times 0.17^{0.121} \times \exp(-0.472 \times 0.128)$$

$$S = 1.432 \text{ cm}$$

According to Sumer and Fredsøe 2002 (Eq. 29),

$$\frac{S}{D} = 0.1 \sqrt{KC} \exp\left(-0.6 \frac{e}{D}\right)$$

$$\frac{S}{5} = 0.1 \sqrt{7} \times \exp(-0.6 \times 0.128)$$

$$S = 1.225 \text{ cm}$$

According to Yasa, R (Eq. 30),

$$\frac{S}{D} = 0.1 KC^{0.53} \exp\left(-1.54 \frac{e}{D}\right)$$

$$\frac{S}{5} = 0.1 \times 7^{0.53} \exp(-1.54 \times 0.128)$$

$$S = 1.152 \text{ cm}$$

Since there is not a large difference between the results obtained, the equilibrium scour depth for the given input conditions can be predicted to be in the range of 1.1 – 1.4 cm.

**Case 2b:** For pipe diameter  $D = 5$  cm, assuming that the wave period and seabed characteristics remain constant, taking  $KC$  number = 30, we have,

$$KC = \frac{U \times T}{D}$$

$$30 = \frac{U \times 2.5}{5}$$

Therefore,

$$U = 60 \text{ cm/s}$$

Hence, the input parameters are:

Table 9: Input parameters for  $D = 5$  cm,  $KC = 30$

Sl. No.	Burial depth, $e/D$	Pipe Diameter, $D$ (cm)	Wave Period, $T$ (s)	Current velocity, $U$ (cm/s)	Bed friction velocity, $U_*$ (cm/s)	Shield's parameter, $\theta$	Reynold's number, $Re$	KC number
1	0.128	5	2.5	60	2.2	0.17	$1.6 \times 10^4$	30

Calculating the scour depth using equations 23, 26, 29 and 30 (since they are more accurate than the rest),

According to Etemad-Shahidi et al. (Eq. 23),

$$\frac{S}{D} = 0.105 KC^{0.503} \exp\left(-0.284 \frac{e}{D}\right) \text{ for } e / D \leq 0.145$$

$$\frac{S}{5} = 0.105 \times 30^{0.503} \times \exp(-0.284 \times 0.128)$$

$$S = 2.801 \text{ cm}$$

According to Etemad-Shahidi et al. (Eq. 26),

$$\frac{S}{D} = 0.149 KC^{0.477} \theta^{0.121} \exp\left(-0.472 \frac{e}{D}\right) \text{ for } \theta > 0.064 \text{ and } e / d \leq 0.145$$

$$\frac{S}{5} = 0.149 \times 30^{0.477} \times 0.17^{0.121} \times \exp(-0.472 \times 0.128)$$

$$S = 2.867 \text{ cm}$$

According to Sumer and Fredsøe 2002 (Eq. 29),

$$\frac{S}{D} = 0.1 \sqrt{KC} \exp\left(-0.6 \frac{e}{D}\right)$$

$$\frac{S}{5} = 0.1 \sqrt{30} \times \exp(-0.6 \times 0.128)$$

$$S = 2.536 \text{ cm}$$

According to Yasa, R (Eq. 30),

$$\frac{S}{D} = 0.1 KC^{0.53} \exp\left(-1.54 \frac{e}{D}\right)$$

$$\frac{S}{5} = 0.1 \times 30^{0.53} \times \exp(-1.54 \times 0.128)$$

$$S = 2.49 \text{ cm}$$

Since there is not a large difference between the results obtained, the equilibrium scour depth for the given input conditions can be predicted to be in the range of 2.5 – 2.8 cm.

**Case 3a:** For pipe diameter  $D = 2$  cm, assuming that the wave period and seabed characteristics remain constant, taking  $KC$  number = 45, we have,

$$KC = \frac{U \times T}{D}$$

$$45 = \frac{U \times 3}{2}$$

Therefore,

$$U = 30 \text{ cm/s}$$

Hence, the input parameters are:

Table 10: Input parameters for  $D = 2$  cm,  $KC = 45$

Sl. No.	Burial depth, $e/D$	Pipe Diameter, $D$ (cm)	Wave Period, $T$ (s)	Current velocity, $U$ (cm/s)	Bed friction velocity, $U_*$ (cm/s)	Shield's parameter, $\theta$	Reynold's number, $Re$	KC number
1	0.2	2	3	30	2	0.11	$4.4 \times 10^4$	45

Calculating the scour depth using equations 23, 26, 29 and 30 (since they are more accurate than the rest),

According to Etemad-Shahidi et al. (Eq. 23),

$$\frac{S}{D} = 0.105 KC^{0.503} \exp\left(-0.284 \frac{e}{D}\right) \text{ for } e / D \leq 0.145$$

$$\frac{S}{D} = 0.105 \times 45^{0.503} \times \exp(-0.284 \times 0.2)$$

$$S = 1.346 \text{ cm}$$

According to Etemad-Shahidi et al. (Eq. 26),

$$\frac{S}{D} = 0.149 KC^{0.477} \theta^{0.121} \exp\left(-0.472 \frac{e}{D}\right) \text{ for } \theta > 0.064 \text{ and } e/d \leq 0.145$$

$$\frac{S}{D} = 0.149 \times 45^{0.477} \times 0.11^{0.121} \times \exp(-0.472 \times 0.2)$$

$$S = 1.276 \text{ cm}$$

According to Sumer and Fredsøe 2002 (Eq. 29),

$$\frac{S}{D} = 0.1 \sqrt{KC} \exp\left(-0.6 \frac{e}{D}\right)$$

$$\frac{S}{D} = 0.1 \sqrt{45} \times \exp(-0.6 \times 0.2)$$

$$S = 1.19 \text{ cm}$$

According to Yasa, R (Eq. 30),

$$\frac{S}{D} = 0.1 KC^{0.53} \exp\left(-1.54 \frac{e}{D}\right)$$

$$\frac{S}{D} = 0.1 \times 45^{0.53} \times \exp(-1.54 \times 0.2)$$

$$S = 1.105 \text{ cm}$$

Since there is not a large difference between the results obtained, the equilibrium scour depth for the given input conditions can be predicted to be in the range of 1.1 – 1.3 cm.

**Case 3b:** For pipe diameter  $D = 2$  cm, assuming that the wave period and seabed characteristics remain constant, taking  $KC$  number = 75, we have,

$$KC = \frac{U \times T}{D}$$

$$75 = \frac{U \times 3}{2}$$

Therefore,

$$U = 50 \text{ cm/s}$$

Hence, the input parameters are:

Table 11: Input parameters for  $D = 2$  cm,  $KC = 45$

Sl. No.	Burial depth, $e/D$	Pipe Diameter, $D$ (cm)	Wave Period, $T$ (s)	Current velocity, $U$ (cm/s)	Bed friction velocity, $U_*$ (cm/s)	Shield's parameter, $\theta$	Reynold's number, $Re$	KC number
1	0.2	2	3	50	2	0.11	$4.4 \times 10^4$	475

Calculating the scour depth using equations 23, 26, 29 and 30 (since they are more accurate than the rest),

According to Etemad-Shahidi et al. (Eq. 23),

$$\frac{S}{D} = 0.105 KC^{0.503} \exp\left(-0.284 \frac{e}{D}\right) \text{ for } e/D \leq 0.145$$

$$\frac{S}{2} = 0.105 \times 75^{0.503} \times \exp(-0.284 \times 0.2)$$

$$S = 1.741 \text{ cm}$$

According to Etemad-Shahidi et al. (Eq. 26),

$$\frac{S}{D} = 0.149 KC^{0.477} \theta^{0.121} \exp\left(-0.472 \frac{e}{D}\right) \text{ for } \theta > 0.064 \text{ and } e/d \leq 0.145$$

$$\frac{S}{2} = 0.149 \times 75^{0.477} \times 0.11^{0.121} \times \exp(-0.472 \times 0.2)$$

$$S = 1.628 \text{ cm}$$

According to Sumer and Fredsøe 2002 (Eq. 29),

$$\frac{S}{D} = 0.1 \sqrt{KC} \exp\left(-0.6 \frac{e}{D}\right)$$

$$\frac{S}{2} = 0.1 \sqrt{75} \times \exp(-0.6 \times 0.2)$$

$$S = 1.536 \text{ cm}$$

According to Yasa, R (Eq. 30),

$$\frac{S}{D} = 0.1 KC^{0.53} \exp\left(-1.54 \frac{e}{D}\right)$$

$$\frac{S}{2} = 0.1 \times 75^{0.53} \times \exp(-1.54 \times 0.2)$$

$$S = 1.449 \text{ cm}$$

Since there is not a large difference between the results obtained, the equilibrium scour depth for the given input conditions can be predicted to be in the range of 1.45 – 1.7 cm.

The variation of equilibrium scour depth with respect to  $KC$  number is as shown below:

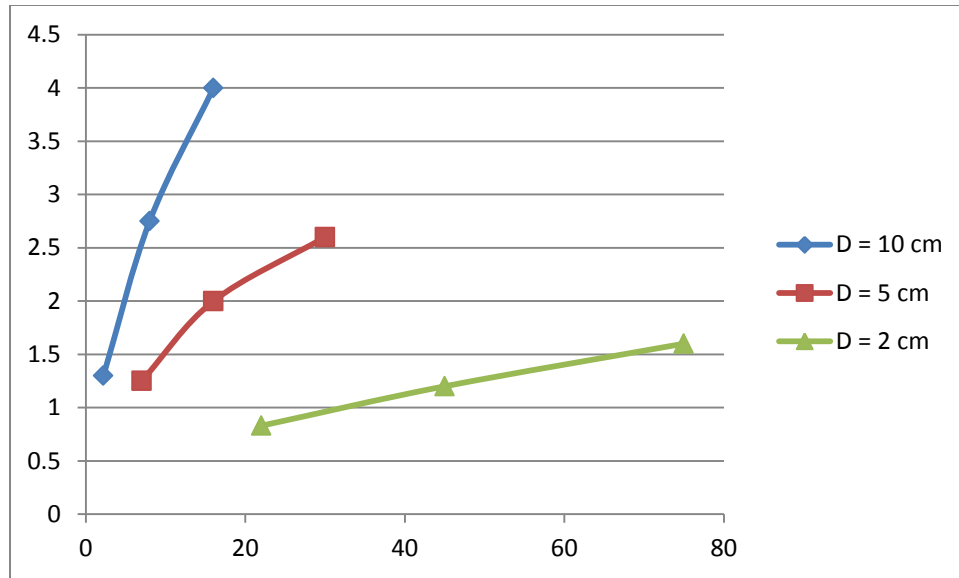


Fig. 5.1: Equilibrium Scour Depth v/s  $KC$  number

From Fig. 5.1, it is evident that the equilibrium scour depth increases with an increase in  $KC$  number. Also, the variation depends on the pipeline diameter, and the increase is more significant at bigger diameters. Thus, minimization of the equilibrium scour depth can be achieved by minimizing the  $KC$  number.  $KC$  number is given by the formula:

$$KC = \frac{U \times T}{D}$$

Where,

$KC$  = Keulegan – Carpenter number

$U$  = Current velocity

$T$  = Time period of wave

$D$  = Pipeline Diameter

Thus, for a given pipeline diameter, the  $KC$  number can be minimized by minimizing the current velocity and/or the time period. These are the main parameters which need to be controlled in order to minimize the equilibrium scour depth.

## CHAPTER 6: CONCLUSIONS AND RECOMMENDATIONS

The research work carried out previously in the field of prediction of scour depth below submarine pipelines has been thoroughly reviewed to have a basic understanding of the scour and self-burial process. The experimental findings of equilibrium scour depth of a pipeline have been compared with the results obtained from each empirical equation suggested by various researchers as per their findings. The most accurate methods of predicting the scour depth have been obtained.

Additionally, the equilibrium scour depth has been calculated for the given diameters with different parameter values. It was found that the equilibrium scour depth increases with an increase in  $KC$  number, but the increase is also governed by the pipe diameter. The increase in equilibrium scour depth is more prominent for large diameters of pipeline. For smaller pipeline diameters, the equilibrium scour depth still increases with increase in  $KC$  number, but this increase is marginal.

The parameters which are more dominant in governing the equilibrium scour depth have been identified. Future work can be carried out to minimize the equilibrium scour depth by subsequent minimization of those parameters.

The empirical formulae and experimental data are valid only for  $KC < 100$ . For  $KC > 100$ , more research has to be carried out.

Also, the experiments assume that the pipeline is rigidly fixed onto the seabed, with some initial embedment. This may not be the case in actual conditions, as the pipeline may be under the influence of vibrations either due to the flow of fluid through it, or due to the water currents around it (vortex-induced vibrations). Such vibrations also have an impact on the scouring process below the pipeline. Future research should be carried out in order to assess the scour depth around a vortex-induced vibrating pipeline.

## REFERENCES

- [1] Sumer BM, Truelsen C, Sichmann T, Fredsøe J. Onset of scour below pipelines and self-burial. *Coastal Engineering* 2001;42: 313–35.
- [2] Mao, Y., 1986. The interaction between a pipeline and an erodible bed. Series Paper 39, Tech. Univ. of Denmark, ISVA, in partial fulfillment of the requirement for the degree of Doctor of Philosophy.
- [3] Sumer BM, Fredsøe J. The mechanics of scour in the marine environment. Singapore: World Scientific; 2002.
- [4] Mao, Y. (1988). "Seabed scour under pipelines." *Proc. 7th Int. Conf. on Offshore and Arctic Engrg.*, Houston, Tex., 33-38.
- [5] Yuksel, Y., Athl, V., and Cevik, E. (1995). "Flow field along a flat surface with a parallel placed cylinder." *Proc., 5th Int. Offshore and Polar Engrg. Conf.*, International Society of Offshore and Polar Engineering, Golden, Colo., 157–161
- [6] Jensen, B. L., Sumer, B. M., Jensen, H. R., and Fredsøe, J. (1990). "Flow around and forces on a pipeline near a scoured bed in steady stream." *J. Offshore Mech. and Arctic Engrg.*, 112, 206–312.
- [7] Fredsøe, J., Hansen, E.A., Mao, Y., Sumer, B.M., 1988. Three-dimensional scour below pipelines. *J. Offshore Mech. Arctic Eng.*, Am. Soc. Mech. Eng. 110, 373–379.
- [8] Chiew YM. Mechanics of local scour around submarine pipelines. *Journal of Hydraulic Engineering*, ASCE 1990;116:515–29.
- [9] Sumer, B.M., Fredsøe, J., 1991. Onset of scour below a pipeline exposed to waves. *Int. J. Offshore Polar Eng.* 1 (3), 189–194.
- [10] Lucassen RJ. Scour underneath submarine pipelines. MATs rep. PL-4 2A. Marine tech. res., The Netherlands. 1984.
- [11] Sumer, B.M., Fredsøe, J., 1997. *Hydrodynamics Around Cylindrical Structures*. World Scientific, xviii + 530 pp.
- [12] van Ast, W. and de Boer, P. L., 1973. *Scour Underneath a Pipeline due to Current and/or Waves*. Delft University of Technology, Coastal Engineering Group [in Dutch]

- [13] Bijker, E. W., 1976. Wave-seabed-structure interaction. *Proc. BOSS Cont.* Pp. 830-844.
- [14] Sumer et. al., 1990. Three-dimensional scour below pipelines. *J. Offshore Mech. Arctic Eng., Am. Soc. Mech. Eng.* 110, 373–379
- [15] Fredsøe, J., Sumer, B.M., Arnskov, M.M., 1992. Time scale for wave / current scour below pipelines. *Int. J. Offshore Polar Eng.* 2 (1), 13–17.
- [16] Chao, J. L., and Hennessy, P. V. (1972). "Local scour under ocean outfall pipelines." *J. Water Pollution Control Federation*, 44(7), 1443-1447.
- [17] Kjeldsen, S. P., GjØrsvik, O., Bringaker, K. G., and Jacobsen, J. (1973). "Local scour near offshore pipelines." *Proc. 2nd Int. Conf. on Port and Oc. Engrg. Under Arctic Conditions*, University of Iceland, 308-331.
- [18] Littlejohns, P. S. G. (1977). "A study of scour around submarine pipelines." *Report No. INT 113*, Hydr. Res. Station, Wallingford, England
- [19] Herbich, J. B. (1981). "Scour around pipelines and other objects." *Offshore pipeline design elements*, Marcell Dekker, Inc., New York, N.Y., 43-96.
- [20] Bijker, E. W., and Leeuwestein, W. (1984). "Interaction between pipelines and the seabed under the influence of waves and currents." *Seabed Mechanics, Proc. Symp. IUTAM/IUGG. International Union of Theoretical Applied Mechanics/International Union of Geology and Geophysics*, 235-242.
- [21] Leeuwenstein, W., Bijker, E.A., Peerbolte, E.B., Wind, H.G., 1985. The natural self-burial of submarine pipelines. *Proc. 4<sup>th</sup> International Conf. on Behavior of Offshore Structures (BOSS)*, vol. 2. Elsevier, pp. 717–728.
- [22] Ibrahim, A., and Nalluri, C. (1986). "Scour prediction around marine pipelines." *Proc. 5th Int. Symp. on Offshore Mech. and Arctic Engrg.*, Tokyo, Japan, 679-684.
- [23] Etemad-Shahidi, A., Yasa, R., & Kazeminezhad, M. H. (2011). Prediction of wave-induced scour depth under submarine pipelines using machine learning approach. *Applied Ocean Research*, 33(1), 54-59.
- [24] Yasa, R. (2011). Prediction of the scour depth under submarine pipelines in wave condition. *Journal of Coastal Research, Special Issue*, 64, 627-630.

- [25] Hulsbergen, C. H. (1984). "Stimulated self-burial of submarine pipelines." *Proc. 16th Offshore Tech. Conf.*, Houston, Tex., 171-175.
- [26] Angus, N. M., & Moore, R. L. (1982). Scour repair methods in the Southern North Sea. *paper OTC, 4410*, 3-6.
- [27] Watson, T. N. (1974). Scour in the North Sea. *J. Pet. Technol.:(United States)*,26.
- [28] Posey, C. J. "Protection against Underscour". Paper OTC 485 presented at the Second Annual Offshore Technology Conference, Houston, Texas, April.22-24, 1970. 11 747-748.
- [29] Hansen, E.A., Staub, C., Fredsøe, J., Sumer, B.M., 1991. Time development of scour induced free spans of pipelines. Proc. 10th Offshore Mechanics and Arctic Engineering Conference, ASME, Stavanger, Norway. Pipeline Technology, vol. 5, pp. 25–31
- [30] Terzaghi, K., 1948. Theoretical Soil Mechanics. Wiley, New York.
- [31] Sumer, B.M., Fredsøe, J., 1994. Self-burial of pipelines at span shoulders. *Int. J. Offshore Polar Eng.* 4 (1), 30–35.
- [32] Sumer, B.M., Fredsøe, J., 1999. Wave Scour Around Structures. In: Liu, P.L.-F. (Ed.), *Advances in Coastal and Ocean Engineering*, vol. 4. World Scientific, Chapter, 51 pp.

## APPENDIX I

Calculation of percentage error:

Case 1: For pipe diameter  $D = 10$  cm

Table 12: Calculation of percentage error for Case 1:  $D = 10$  cm

Sl. No	Formula	Value from empirical formula	Experimental value	Percentage error = $\left(\frac{ Calc. value - Expt. value }{Experimental value}\right) \times 100$	% Error
1	Kjeldsen et al.	1.448	1.3	$= \left(\frac{ 1.448 - 1.3 }{1.3}\right) \times 100$	11.38
2	Sumer et al.	1.483		$= \left(\frac{ 1.483 - 1.3 }{1.3}\right) \times 100$	14.08
3	Ibrahim and Nalluri	1.39		$= \left(\frac{ 1.39 - 1.3 }{1.3}\right) \times 100$	6.92
4	Etemad-Shahidi et al.	1.547		$= \left(\frac{ 1.547 - 1.3 }{1.3}\right) \times 100$	19
5	Etemad-Shahidi et al. (with Shield's parameter)	1.39		$= \left(\frac{ 1.39 - 1.3 }{1.3}\right) \times 100$	6.92
6	Sumer and Fredsøe	1.422		$= \left(\frac{ 1.422 - 1.3 }{1.3}\right) \times 100$	9.38
7	Yasa R	1.364		$= \left(\frac{ 1.364 - 1.3 }{1.3}\right) \times 100$	4.92
8	Bijker and Leeuwestein	1.2103		$= \left(\frac{ 1.2103 - 1.3 }{1.3}\right) \times 100$	6.9

Case 2: For pipe diameter  $D = 5$  cm

Table 13: Calculation of percentage error for Case 2:  $D = 5$  cm

Sl. No	Formula	Value from empirical formula	Experimental value	Percentage error = $\left(\frac{ Calc. value - Expt. value }{Experimental value}\right) \times 100$	% Error
1	Kjeldsen et al.	1.22	2.0	$= \left(\frac{ 1.22 - 2.0 }{2.0}\right) \times 100$	39
2	Sumer et al.	2.0		$= \left(\frac{ 2.0 - 2.0 }{2.0}\right) \times 100$	0
3	Ibrahim and Nalluri	1.38		$= \left(\frac{ 1.38 - 2.0 }{2.0}\right) \times 100$	31
4	Etemad-Shahidi et al.	2.042		$= \left(\frac{ 2.042 - 2.0 }{2.0}\right) \times 100$	2.1
5	Etemad-Shahidi et al. (with Shield's parameter)	2.124		$= \left(\frac{ 2.124 - 2.0 }{2.0}\right) \times 100$	6.2
6	Sumer and Fredsøe	1.85		$= \left(\frac{ 1.85 - 2.0 }{2.0}\right) \times 100$	7.5
7	Yasa R	1.785		$= \left(\frac{ 1.785 - 2.0 }{2.0}\right) \times 100$	10.75
8	Bijker and Leeuwestein	1.57		$= \left(\frac{ 1.57 - 2.0 }{2.0}\right) \times 100$	21.5

Case 3: For pipe diameter  $D = 2$  cm

Table 14: Calculation of percentage error for Case 3:  $D = 2$  cm

Sl. No	Formula	Value from empirical formula	Experimental value	Percentage error = $\left(\frac{ Calc. value - Expt. value }{Experimental value}\right) \times 100$	% Error
1	Kjeldsen et al.	0.343	0.83	$= \left(\frac{ 0.343 - 0.83 }{0.83}\right) \times 100$	58.67
2	Sumer et al.	0.938		$= \left(\frac{ 0.938 - 0.83 }{0.83}\right) \times 100$	13.01
3	Ibrahim and Nalluri	1.42		$= \left(\frac{ 1.42 - 0.83 }{0.83}\right) \times 100$	71
4	Etemad-Shahidi et al.	0.912		$= \left(\frac{ 0.912 - 0.83 }{0.83}\right) \times 100$	9.88
5	Etemad-Shahidi et al. (with Shield's parameter)	0.907		$= \left(\frac{ 0.907 - 0.83 }{0.83}\right) \times 100$	9.277
6	Sumer and Fredsøe	0.832		$= \left(\frac{ 0.832 - 0.83 }{0.83}\right) \times 100$	0.241
7	Yasa R	0.756		$= \left(\frac{ 0.756 - 0.83 }{0.83}\right) \times 100$	8.916
8	Bijker and Leeuwestein	0.542		$= \left(\frac{ 0.542 - 0.83 }{0.83}\right) \times 100$	34.7